Evolutionary Multimodal Multiobjective Optimization for Traveling Salesman Problems {Supplementary Material}

Yiping Liu, *Member, IEEE*, Liting Xu, Yuyan Han, Xiangxiang Zeng, Gary G. Yen, *Fellow, IEEE*, and Hisao Ishibuchi, *Fellow, IEEE*

This is the supplementary material of the paper entitled "Evolutionary Multimodal Multiobjective Optimization for Traveling Salesman Problems." It contains the following items:

- Section S-I gives the proofs of Statements 1, 2, and 3 in Section III of the paper.
- Section S-II analyzes the running time of EAX-W and EAX-ND.
- Section S-III investigates the effect of the population size on the performance of TSPXEA.
- Section S-IV discusses how TSPXEA achieves the balance between the diversity in the objective and decision spaces.
- Section S-V shows the visualized results of the solution sets obtained by the compared algorithms.
- Section S-VI shows the convergence plots towards true Pareto fronts obtained by the compared algorithms.
- Section S-VII explains why the GD values obtained by TSPXEA are not always the best on small-scale problems.
- Section S-VIII shows the effect of an unlimited archive for MMTSPs.
- Section S-IX discusses the characteristics of the test problems.
- Section S-X shows the results obtained by the compared algorithms on the 'R' series test problems.
- Section S-XI investigates the performance of TSPXEA on multimodal single-objective TSPs.
- Section S-XII contains the additional figures and tables mentioned in the paper.

S-I. Proofs of Statements 1, 2, and 3

Proof of Statement 1. Define an edge that links a C-type vertex and a D-type vertex as e^{CD}. Define an edge that is e^{CD} but neither (c_1, d_1) nor (c_2, d_2) as $\tilde{e}^{CD}$. Denote an solution that does not satisfy Statement 1 as $\tilde{\boldsymbol{x}}$. That is, $\tilde{\boldsymbol{x}}$ has at least one $\tilde{e}^{CD}$. Statement 1 will be proven if we show that $\tilde{\boldsymbol{x}}$ is not a Pareto optimal solution.

Denote the number of e^{CD} in a solution to the MMTSP as h. h is an even number in $[2, 2k^D]$ (we assume $k_D < k_C$). The mth objective value of $\tilde{\boldsymbol{x}}$ can be formulated as follows.

$$f_m(\tilde{\boldsymbol{x}}) = O_m^C + O_m^D - \sum_{i=1}^{h/2} (l_m(e_i^C) + l_m(e_i^D)) + l_m(e_a) + l_m(e_b) + (h-2) \cdot l_m(\tilde{e}^{CD}). \tag{S.1}$$

We illustrate how to obtain (S.1) in Fig. S.1. The topological circuit of $\tilde{\boldsymbol{x}}$ is shown in Fig. S.1 (a). The paths that link C-type vertices are in blue, and those link D-type vertices are in green. e^{CD} of $\tilde{\boldsymbol{x}}$ are red lines. We only show four of them for concise illustration (i.e., $h = 4$). They are e_a, e_b, and two $\tilde{e}^{CD}$. At least one of e_a and e_b is $\tilde{e}^{CD}$. In Fig. S.1 (b), we reomove all e^{CD} of $\tilde{\boldsymbol{x}}$. Then we add some edges between C-type vertices to form a Hamiltonian circuit for all C-type vertices. Those edges are denoted as $e_i^C, i = 1, \ldots, h/2$ (blue dotted lines). Similarly, we add edges $e_i^D, i = 1, \ldots, h/2$ (green dotted lines) to form a Hamiltonian circuit for all D-type vertices. O_m^C and O_m^D are the lengths of the Hamiltonian circuits corresponding to the mth objective. Then, we have $f_m(\tilde{\boldsymbol{x}})$ in (S.1) by removing and adding edges based on the Hamiltonian circuits.

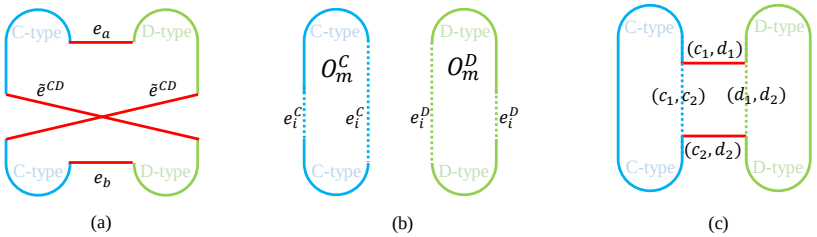

Fig. S.1. (a) Solution $\tilde{\boldsymbol{x}}$ that not satisfies Statement 1. (b) Two Hamiltonian circuits of C-type and D-type vertices, respectively. They are obtained by removing some edges in $\tilde{\boldsymbol{x}}$ and adding some edges between C-type (D-type) vertices. (c) Solution $\bar{\boldsymbol{x}}$ that shares the same circuits in (b) and satisfies Statement 1. We prove that $\tilde{\boldsymbol{x}}$ is not a Pareto optimal solution since it is dominated by $\bar{\boldsymbol{x}}$.

There exsits a solution $\bar{\boldsymbol{x}}$ that shares the Hamiltonian circuits in Fig. S.1 (b), and it contains edges (c_1, d_1) and (c_2, d_2) but no $\tilde{e}^{CD}$. That is, we can remove edges (c_1, c_2) and (d_1, d_2) from the Hamiltonian circuits and add edges (c_1, d_1) and (c_2, d_2) to obtain $\bar{\boldsymbol{x}}$, which is shown in Fig. S.1 (c). Then the mth objective value of $\bar{\boldsymbol{x}}$ is calculated by the following equation.

$$f_m(\bar{\boldsymbol{x}}) = O_m^C + O_m^D - l_m(c_1, c_2) - l_m(d_1, d_2) + l_m(c_1, d_1) + l_m(c_2, d_2). \tag{S.2}$$

For $m = 1, \ldots, M$, since the values of $l_m(c_1, d_1)$, $l_m(c_2, d_2)$, $l_m(c_1, c_2)$, $l_m(d_1, d_2)$, $l_m(e_i^C)$, and $l_m(e_i^D)$ are in $[0, l_{\max}]$, and the values of $l_m(\tilde{e}^{CD})$ are in $(3l_{\max}, 4l_{\max})$, we have $f_m(\tilde{\boldsymbol{x}}) > f_m(\bar{\boldsymbol{x}})$. Therefore, $f_m(\tilde{\boldsymbol{x}})$ is dominated by $f_m(\bar{\boldsymbol{x}})$, and $\tilde{\boldsymbol{x}}$ cannot be a Pareto optimal solution. We have thus proved the statement. □

Proof of Statement 2. Denote a solution that satisfies Statement 1 but not Statement 2 as $\check{\boldsymbol{x}} = (c_1, \check{x}_2, \ldots, \check{x}_{k^C-1}, c_2, d_2, \check{x}_{k^C+2}, \check{x}_{k^C+3}, \ldots, \check{x}_{n-1}, d_1, c_1)$, where $(\check{x}_2, \ldots, \check{x}_{k^C-1}) \neq (x_2^S, \ldots, x_{k^C-1}^S)$. Statement 2 will be proven if we show that $\check{\boldsymbol{x}}$ is not a Pareto optimal solution.

There exists a solution $\hat{\boldsymbol{x}}$ that not only satisfies Statements 1 and 2 but also shares the same path for D-type vertices as $\check{\boldsymbol{x}}$. That is, $\hat{\boldsymbol{x}} = (c_1, x_2^S, \ldots, x_{k^C-1}^S, c_2, d_2, \check{x}_{k^C+2}, \check{x}_{k^C+3}, \ldots, \check{x}_{n-1}, d_1, c_1)$. For the mth objective, we have

$$\begin{aligned} f_m(\check{\boldsymbol{x}}) &= f^S(\check{\boldsymbol{x}}^S) - l_m(c1, c2) + \check{O}_m, \\ f_m(\hat{\boldsymbol{x}}) &= f^S(\boldsymbol{x}^S) - l_m(c1, c2) + \check{O}_m, \end{aligned} \tag{S.3}$$

where $\check{\boldsymbol{x}}^S = (c_1, \check{x}_2, \check{x}_3, \ldots, \check{x}_{k^C-1}, c_2, c_1)$ is a solution to the single-objective TSP, $f^S(\check{\boldsymbol{x}}^S)$ and $f^S(\boldsymbol{x}^S)$ are the objective values of $\check{\boldsymbol{x}}^S$ and $\boldsymbol{x}^S$ for the single-objective TSP, respectively, and $\check{O}_m$ is the length of $(c_2, d_2, \check{x}_{k^C+2}, \check{x}_{k^C+3}, \ldots, \check{x}_{n-1}, d_1, c_1)$ corresponding to the mth objective. $\check{\boldsymbol{x}}^S$ cannot be an optimal solution to the single-objective TSP since it contains edge (c_1, c_2) (refer to Algorithm 2, line 2). We can see that $f_m(\check{\boldsymbol{x}}) > f_m(\hat{\boldsymbol{x}})$ since $f^S(\check{\boldsymbol{x}}^S) > f^S(\boldsymbol{x}^S)$. $\check{\boldsymbol{x}}$ is dominated by $\hat{\boldsymbol{x}}$. That is, $\check{\boldsymbol{x}}$ cannot be a Pareto optimal solution. We have thus proved the statement. □

Proof of Statement 3. When $p_c = 1$, for a solution $\boldsymbol{x}$ that satisfies Statements 1 and 2, we have

$$\begin{aligned} \sum_{m=1}^{M} f_m(\boldsymbol{x}) &= \sum_{m}^{M} \{ \sum_{i=1}^{n-1} l_m(x_i, x_{i+1}) + l_m(x_1, x_n) \} \\ &= C_1 + C_2 + C_3, \end{aligned} \tag{S.4}$$

where

$$C_1 = M \cdot f^S(\boldsymbol{x}^S) - M \cdot l_1(c_1, c_2), \tag{S.5}$$

$$C_2 = \sum_{m}^{M} \{ l_m(c_1, d_1) + l_m(c_2, d_2) \}, \tag{S.6}$$

$$C_3 = \sum_{i=k_C+1}^{n-1} \sum_{m}^{M} l_m(x_i, x_{i+1}) = (k_D - 1) \cdot p_s. \tag{S.7}$$

Please refer to lines 4-6 and 23 in Algorithm 1 for calculating C_3. Because C_1, C_2, and C_3 are constant values, $\sum_{m=1}^{M} f_m(\boldsymbol{x})$ is a constant value. This means that $\boldsymbol{x}$ is on a hyperplane in the objective space defined by (S.4). All the solutions on the hyperplane are non-dominated by each other. Therefore, all the possible solutions that satisfy Statements 1 and 2 are Pareto optimal solutions. The number of these solutions is $(k_D - 2)!$. We have thus proved the statement. □

S-II. Running time of EAX-W and EAX-ND

Let us denote TSPXEA with only EAX-W and EAX-ND as TSPXEA-W and TSPXEA-ND, respectively. We compare the running time of TSPXEA-W and TSPXEA-ND to solve MMTSPs at different scales with different population sizes in this section.

Fig. S.2 shows the average running time over 30 runs of TSPXEA-W and TSPXEA-ND in solving uni1+D1, bays29+D1, att48+D1, lin105+D1, and a280+D1. Note that the vertical axis of the figure has a log-scale. The scales of these problems increase gradually. Note that the population size N is set to 100, and the stopping criterion is set when the number of evaluated solutions reaches $50,000$. We can see from Fig. S.2 that in uni1+D1, the running time of TSPXEA-W and TSPXEA-ND is similar, and TSPXEA-W even runs slightly longer than TSPXEA-ND does. On the other test problems, TSPXEA-ND consumes more time than TSPXEA-W does. As the scale of the problem increases, the difference in the running time between TSPXEA-W and TSPXEA-ND also increases dramatically.

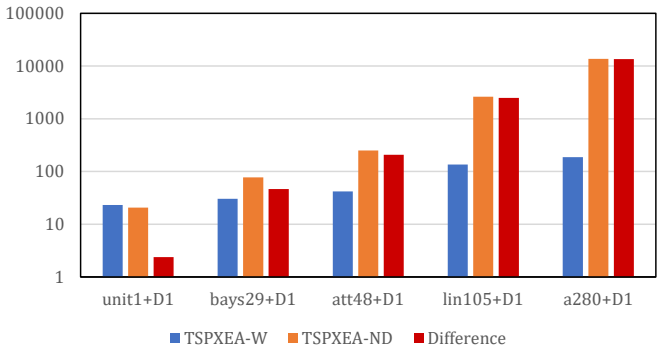

Fig. S.2. The average running time (seconds) over 30 tuns of TSPXEA-W and TSPXEA-ND on solving problems with different scales. Note that the vertical axis of the figure has a log-scale.

Fig. S.3 shows the average running time over 30 runs of TSPXEA-W and TSPXEA-ND in solving att48+D1 when the population size is 100, 300, 600, and 1,000. Note that the vertical axis of the figure has a log-scale, and the stopping criterion is set when the number of evaluated solutions reaches $50,000$. We can see from Fig. S.3 that TSPXEA-ND consumes more time than TSPXEA-W does in all cases. As the population size increases, the difference in the running time between TSPXEA-W and TSPXEA-ND also increases.

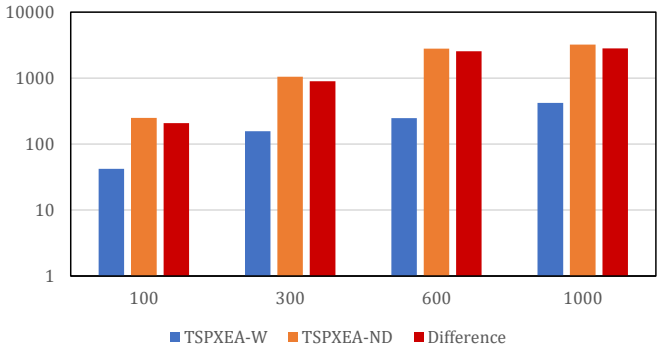

Fig. S.3. The average running time (seconds) over 30 tuns of TSPXEA-W and TSPXEA-ND with different population sizes. Note that the vertical axis of the figure has a log-scale.

Based on the above observations, we can conclude that the running time of both TSPXEA-W and TSPXEA-ND is affected by the problem scale and the population size. However, TSPXEA-W is much less affected than TSPXEA-ND and usually runs much faster than TSPXEA-ND.

S-III. The Effect of the Population Size

This section investigates the effect of the population size on the performance of the proposed algorithm TSPXEA. We apply TSPXEA to solve uni1+D1-D10 when the population size is 100, 300, 600, and 1000, denoted as TSPXEA_100, TSPXEA_300, TSPXEA_600, and TSPXEA_1000, respectively. The stop criterion is the number of evaluated solutions reaches $50,000$.

Table S.I shows the average IGDM, HV, and GD values over 30 runs and the corresponding performance scores obtained by TSPXEA with different population sizes. The performance score of TSPXEA with a specific choice of population size is the number where it statistically significantly outperforms the other designs with respect to a performance indicator. Taking the results of IGDM in uni1+D1 as an example, TSPXEA_100 dose not perform statistically significant better than any other designs. TSPXEA_300 statistically significantly outperforms the other three, while TSPXEA_600 statistically significantly outperforms TSPXEA_100 and TSPXEA_1000. The case of TSPXEA_1000 is the same as that of TSPXEA_100. Therefore, for uni+D1, the performance scores are 0, 3, 2, and 0 for TSPXEA_100, TSPXEA_300, TSPXEA_600 and TSPXEA_1000, respectively. The average performance score (APS for short) refers to the average value of the performance scores among all test problems. We can see from Table S.I that TSPXEA_300 generally obtains the best IGDM, HV, and GD according to the average performance scores. On the other hand, TSPXEA_100 acquires the second best HV and GD and the second worst IGDM. The performance of TSPXEA_600 is often in the middle among these designs. TSPXEA_1000 is considered the worst design according to all indicators.

TABLE S.I
THE AVERAGE IGDM, HV, AND GD VALUES OVER 30 RUNS AND THE CORRESPONDING PERFORMANCE SCORES OBTAINED BY TSPXEA WITH DIFFERENT POPULATION SIZES.

	IGDM								HV								GD							
	TSPXEA_100		TSPXEA_300		TSPXEA_600		TSPXEA_1000		TSPXEA_100		TSPXEA_300		TSPXEA_600		TSPXEA_1000		TSPXEA_100		TSPXEA_300		TSPXEA_600		TSPXEA_1000	
uni1+D1	8.047E-3	0	3.290E-3	3	5.812E-3	2	8.094E-3	0	9.951E-1	2	9.967E-1	3	9.936E-1	1	9.904E-1	0	3.715E-4	2	2.628E-4	3	4.474E-4	1	6.947E-4	0
uni1+D2	1.637E-2	0	6.511E-3	3	1.098E-2	2	1.354E-2	1	9.828E-1	0	9.921E-1	3	9.832E-1	1	9.784E-1	0	1.637E-3	0	8.498E-4	3	2.129E-3	0	2.719E-3	0
uni1+D3	4.302E-3	2	4.108E-3	2	6.332E-3	1	7.633E-3	0	9.984E-1	3	9.878E-1	2	9.816E-1	1	9.760E-1	0	9.684E-5	3	1.572E-3	2	1.944E-3	0	2.094E-3	0
uni1+D4	1.057E-2	0	6.335E-3	3	8.867E-3	2	9.604E-3	1	9.928E-1	3	9.904E-1	2	9.851E-1	0	9.851E-1	0	6.396E-4	0	4.323E-4	2	4.397E-4	2	5.028E-4	1
uni1+D5	1.050E-2	0	4.536E-3	3	7.587E-3	2	9.355E-3	1	9.929E-1	2	9.924E-1	2	9.857E-1	1	9.822E-1	0	1.739E-4	2	2.074E-4	2	5.165E-4	0	5.507E-4	0
uni1+D6	8.827E-3	1	7.475E-3	2	8.168E-3	1	1.001E-2	0	9.931E-1	3	9.913E-1	2	9.896E-1	1	9.860E-1	0	1.934E-4	3	8.980E-4	2	1.036E-3	1	1.144E-3	0
uni1+D7	7.211E-3	3	8.218E-3	2	9.304E-3	1	1.122E-2	0	9.917E-1	3	9.818E-1	2	9.756E-1	0	9.713E-1	0	4.585E-4	3	4.849E-4	0	5.898E-4	0	5.731E-4	0
uni1+D8	8.112E-3	0	2.393E-3	3	3.635E-3	2	7.681E-3	0	9.926E-1	1	9.966E-1	3	9.931E-1	1	9.840E-1	0	2.383E-4	1	3.911E-5	3	1.333E-4	2	5.673E-4	0
uni1+D9	8.879E-3	0	2.980E-3	3	4.827E-3	2	7.467E-3	1	9.934E-1	2	9.950E-1	2	9.891E-1	1	9.809E-1	0	0.000E+0	3	4.091E-5	2	1.808E-4	1	2.271E-4	0
uni1+D10	9.064E-3	0	2.259E-3	3	3.714E-3	2	5.609E-3	1	9.936E-1	1	9.980E-1	3	9.915E-1	1	9.862E-1	0	1.348E-5	2	3.046E-5	2	2.106E-4	1	3.457E-4	0
APS	0.6		2.7		1.7		0.5		2		2.4		0.8		0		1.9		2.1		0.8		0.1	

There are two main reasons for these observations. First, a larger population usually leads to better values of IGDM and HV since a larger population usually implies a better diversity. This is why TSPXEA_300 outperforms TSPXEA_100. However, the other reason is that an overly large population size (such as 600 and 1000) can slow down the convergence due to a small number of generations under the termination condition of the same number of examined solutions. That is, the poor GD values obtained by TSPXEA_600 and TSPXEA_1000 result in their poor IGDM and HV values. We observe that the population of TSPXEA_1000 is often sorted into several non-dominated fronts, while TSPXEA_100 usually has one front. Every solution in TSPXEA has an equal probability of being selected in mating selection. Therefore, for a design with a larger population size, solutions are selected not only from the best front (i.e., well-converged solutions) but also from the other fronts (i.e., not well-converged solutions) for generating offspring. Although such a mating selection operator can enhance the diversity of the population, it may result in a poor convergence when the population size is chosen too large.

S-IV. THE BALANCE BETWEEN THE DIVERSITY IN THE OBJECTIVE AND DECISION SPACES

We use Eq. (9) in the environmental selection of TSPXEA to balance the diversity in the objective and decision spaces. $f^K(\boldsymbol{x})$ and $f^E(\boldsymbol{x})$ are two components in Eq. (9), which consider diversity in the objective space and that in the decision space, respectively. In this section, we investigate the performance of TSPXEA when we consider the diversity in the decision space only (i.e., setting $f^K(\boldsymbol{x}) = 0$ in Eq. (9)) and the diversity in the objective space only (i.e., setting $f^E(\boldsymbol{x}) = 0$ in Eq. (9)). The two consequential variants of TSPXEA are denoted as TSPXEA_dec and TSPXEA_obj. We apply them to uni1+D1-D10. The stopping criterion is the number of evaluated solutions reaches $50,000$.

Table S.II shows the average IGDM, HV, GD, Entropy, and Spacing values over 30 runs and the corresponding performance scores obtained by TSPXEA, TSPXEA_dec, and TSPXEA_obj. Here, Entropy evaluates the diversity of a solution set in the decision space (the larger, the better), while Spacing evaluates the diversity of a solution set in the objective space (the smaller, the better). We have the following observations from Table S.II: (1) TSPXEA_dec obtains the best values of Entropy on all test problems, followed by TSPXEA. This observation verifies that the component $f^E(\boldsymbol{x})$ can enhance the diversity in the decision space. (2) TSPXEA_obj obtains the best values of Spacing on most test problems, which indicates that using the component $f^K(\boldsymbol{x})$ contributes to the diversity in the objective space. However, on uni1+D5, D7, and D10, TSPXEA outperforms TSPXEA_obj on Spacing. We speculate that promoting diversity in the decision space may also benefit the diversity in the objective space in some cases. (3) TSPXEA_obj generally obtains the best values of IGDM, HV, and GD, thanks to its good performance in the objective space, whereas TSPXEA_dec performs the worst on these indicators. Note that IGDM is a comprehensive indicator that evaluates a solution set in both the objective and decision spaces. Although TSPXEA considers the diversity in both the objective and decision spaces, the IGDM values obtained by TSPXEA are generally worse than those of TSPXEA_obj since TSPXEA_obj performs very well in the objective space. That is, the diversity maintenance in the decision space has some negative effects on the search for the Pareto front in compared with TSPXEA_obj which focuses only on the objective space.

TABLE S.II
THE AVERAGE IGDM, HV, GD, ENTROPY, AND SPACING VALUES OVER 30 RUNS AND THE CORRESPONDING PERFORMANCE SCORES OBTAINED BY TSPXEA, TSPXEA_DEC, AND TSPXEA_OBJ.

	IGDM						HV						GD						Entropy						Spacing					
	TSPXEA		TSPXEA_dec		TSPXEA_obj		TSPXEA		TSPXEA_dec		TSPXEA_obj		TSPXEA		TSPXEA_dec		TSPXEA_obj		TSPXEA		TSPXEA_dec		TSPXEA_obj		TSPXEA		TSPXEA_dec		TSPXEA_obj	
uni1+D1	8.047E-3	1	1.289E-2	0	6.763E-3	2	9.951E-1	1	9.860E-1	0	9.970E-1	2	3.715E-4	1	7.132E-4	0	3.267E-4	2	3.496E+0	1	3.523E+0	2	3.448E+0	0	1.276E-2	1	1.411E-2	0	1.237E-2	2
uni1+D2	1.637E-2	1	2.650E-2	0	5.792E-3	2	9.828E-1	1	9.663E-1	0	9.970E-1	2	1.637E-3	1	2.076E-3	0	3.397E-4	2	3.356E+0	1	3.367E+0	2	3.241E+0	0	1.638E-2	1	2.460E-2	0	1.205E-2	2
uni1+D3	4.302E-3	1	7.093E-3	0	4.417E-3	1	9.984E-1	1	9.858E-1	0	9.984E-1	1	9.684E-5	1	8.342E-4	0	1.293E-4	1	3.254E+0	1	3.272E+0	2	3.244E+0	0	2.996E-2	0	2.970E-2	0	2.982E-2	1
uni1+D4	1.057E-2	1	1.893E-2	0	8.489E-3	2	9.928E-1	1	9.759E-1	0	9.958E-1	2	6.396E-4	1	1.056E-3	0	4.945E-4	2	3.493E+0	1	3.513E+0	2	3.421E+0	0	1.316E-2	1	1.515E-2	0	1.082E-2	2
uni1+D5	1.050E-2	1	1.548E-2	0	9.053E-3	2	9.929E-1	1	9.828E-1	0	9.959E-1	2	1.739E-4	1	8.085E-4	0	1.281E-5	2	3.393E+0	1	3.411E+0	2	3.329E+0	0	1.895E-2	2	1.933E-2	0	2.120E-2	0
uni1+D6	8.827E-3	1	3.000E-2	0	6.077E-3	2	9.931E-1	1	9.468E-1	0	9.957E-1	2	1.934E-4	1	2.778E-3	0	2.247E-4	1	3.495E+0	1	3.578E+0	2	3.385E+0	0	1.335E-2	1	1.720E-2	0	1.005E-2	2
uni1+D7	7.211E-3	1	1.595E-2	0	7.350E-3	1	9.917E-1	2	9.722E-1	0	9.876E-1	1	4.585E-4	1	6.327E-4	0	5.510E-4	0	3.380E+0	1	3.394E+0	2	3.357E+0	0	1.646E-2	2	2.988E-2	0	2.014E-2	1
uni1+D8	8.112E-3	1	1.259E-2	0	7.922E-3	1	9.926E-1	1	9.816E-1	0	9.932E-1	1	2.383E-4	1	6.840E-4	0	1.196E-4	2	3.533E+0	1	3.551E+0	2	3.469E+0	0	1.290E-2	1	1.434E-2	0	1.257E-2	1
uni1+D9	8.879E-3	2	1.459E-2	0	1.034E-2	1	9.934E-1	2	9.780E-1	0	9.907E-1	1	0.000E+0	2	5.321E-4	0	1.447E-4	1	3.430E+0	1	3.440E+0	2	3.415E+0	0	1.016E-2	1	1.513E-2	0	9.781E-3	2
uni1+D10	9.064E-3	2	1.452E-2	0	1.017E-2	1	9.936E-1	2	9.790E-1	0	9.922E-1	1	1.348E-5	1	6.798E-4	0	6.746E-6	1	3.441E+0	1	3.450E+0	2	3.413E+0	0	8.255E-3	2	1.832E-2	0	8.982E-3	1
APS	1.2		0		1.5		1.3		0		1.5		1.1		0		1.4		1		2		0		1.2		0		1.4	

S-V. VISUALIZATION OF THE SOLUTION SETS OBTAINED BY THE COMPARED ALGORITHMS IN SUBSECTION V-D

Figs. S.4-S.7 show the solution set of a single run in the objective space obtained by each algorithm on uni1+D1, bays29+D1, att48+D1, and lin105+D1, respectively, where a green circle represents a point corresponding to a single solution and a red square represents a point corresponding to multiple solutions. This particular run is associated with the result closest to the mean IGDM value. Note that the scales of the test problems increase gradually. However, their Pareto fronts are the same.

From Fig. S.4, we can see that TSPXEA and DNEA-TSP approximate the Pareto front well, and DNEA-TSP looks slightly better than TSPXEA. However, TSPXEA finds more points with equivalent Pareto optimal solutions than DNEA-TSP does. EGA obtains an acceptable front. It is interesting that although EGA is not designed to maintain diversity in the decision space, it finds several points with equivalent Pareto optimal solutions. DCDG obtains a well-converged front. However, the size of its solution set (i.e., the number of obtained solutions in the solution set) is much smaller than that of the other algorithms. The reason is that DCDG fails to tune the grid size to a proper value on this test problem. In addition, DCDG only finds points with one solution. Some solutions obtained by DYN are far away from the Pareto front, which are outside the objective space $[0, 1] \times [0, 1]$ in each figure in Fig. S.4. The reason is that DYN optimizes an additional objective about diversity in the decision space. Solutions with good values on that objective may have poor values on the original objectives. On the other hand, optimizing the additional objective does not lead to many points with multiple solutions. The solution set obtained by NMA is not well distributed in the objective space. The reason is that different weight vectors often result in the same Pareto optimal solution. The good thing is that most points found by NMA correspond to multiple Pareto optimal solutions.

We can see from Figs. S.5-S.7 that only TSPXEA converges well to the Pareto front and finds points with multiple solutions. The solutions obtained by DCDG are the second closest to the Pareto front. The solution's diversity in the objective space is good. However, there is no point with multiple solutions. Although DNEA-TSP has better convergence performance than EAG, DYN, and NMA, the solutions obtained by the four algorithms are far away from the Pareto front. Besides, the four algorithms occasionally find points with multiple solutions.

According to the intuitive results in Figs. S.4-S.7, TSPXEA is considered the best in searching for equivalent Pareto optimal solutions.

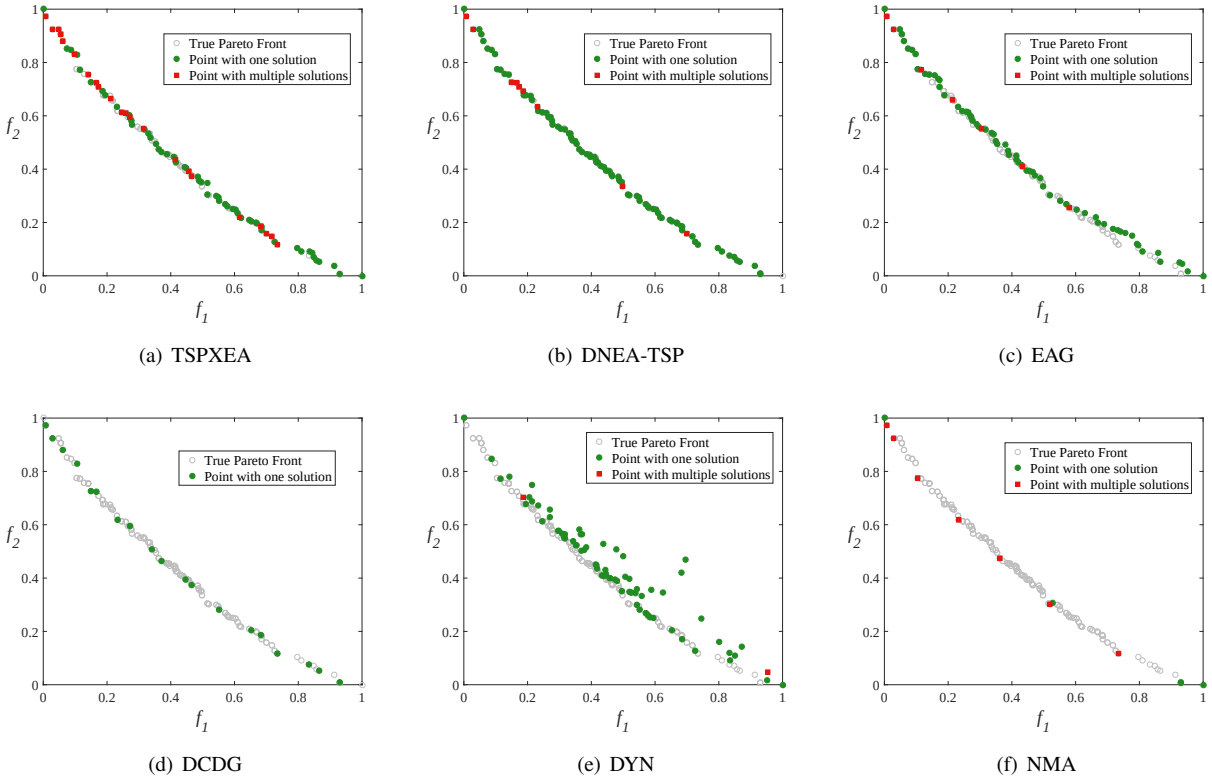

(a) TSPXEA (b) DNEA-TSP (c) EAG

(d) DCDG (e) DYN (f) NMA

Fig. S.4. The solution set of a single run in the objective space obtained by each compared algorithm on uni1+D1. This particular run is associated with the result closest to the mean IGDM value. (a) TSPXEA. (b) DNEA-TSP. (c) EAG. (d) DCDG. (e) DYN. (f) NMA.

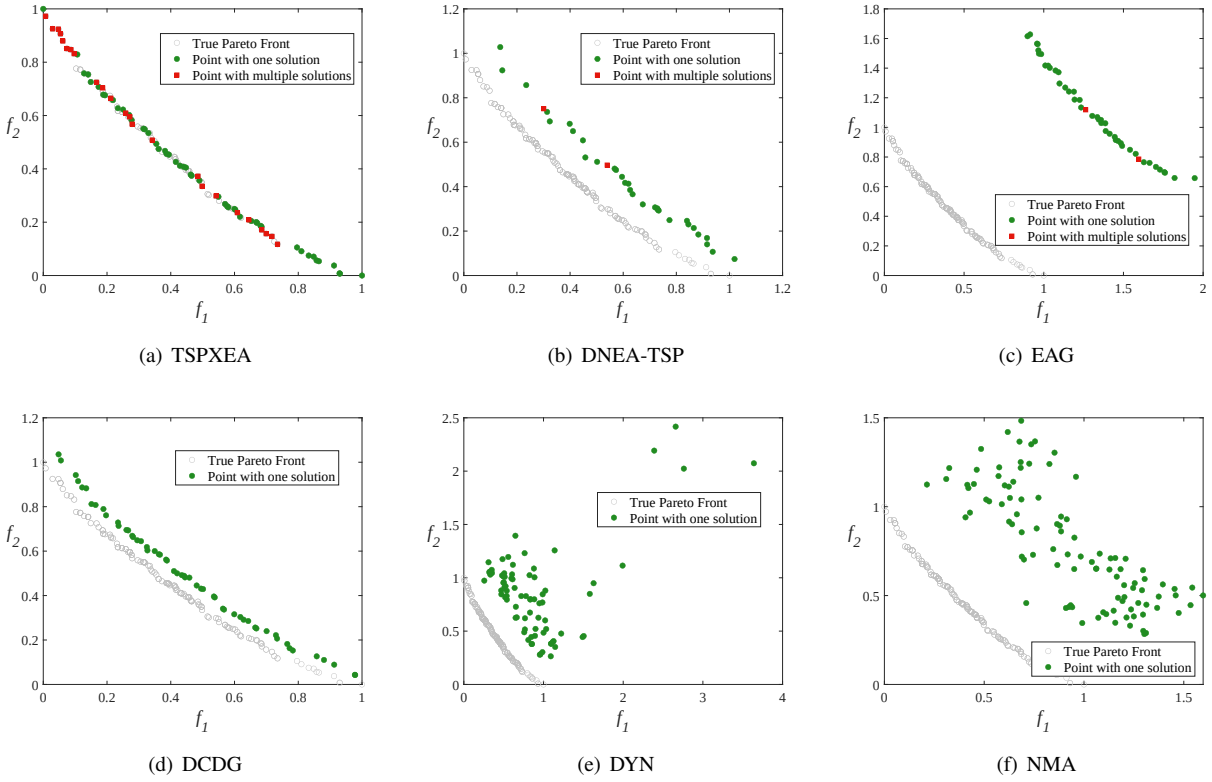

(a) TSPXEA (b) DNEA-TSP (c) EAG

(d) DCDG (e) DYN (f) NMA

Fig. S.5. The solution set of a single run in the objective space obtained by each compared algorithm on bays29+D1. This particular run is associated with the result closest to the mean IGDM value. (a) TSPXEA. (b) DNEA-TSP. (c) EAG. (d) DCDG. (e) DYN. (f) NMA.

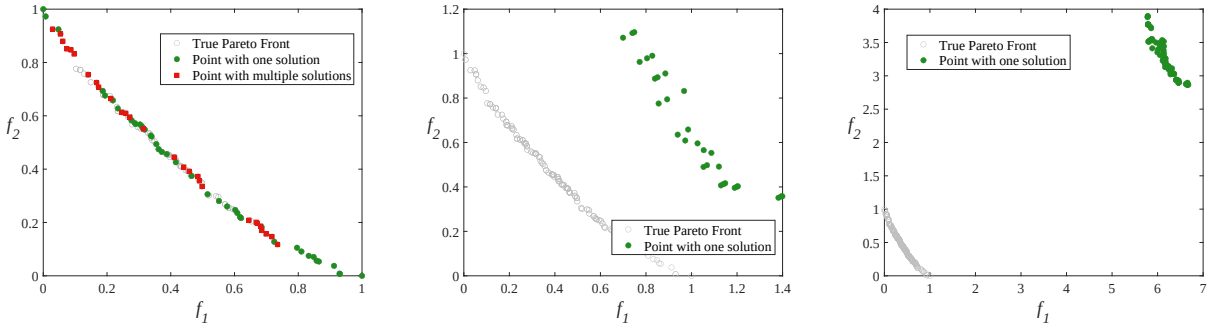

(a) TSPXEA (b) DNEA-TSP (c) EAG

(d) DCDG (e) DYN (f) NMA

Fig. S.6. The solution set of a single run in the objective space obtained by each compared algorithm on att48+D1. This particular run is associated with the result closest to the mean IGDM value. (a) TSPXEA. (b) DNEA-TSP. (c) EAG. (d) DCDG. (e) DYN. (f) NMA.

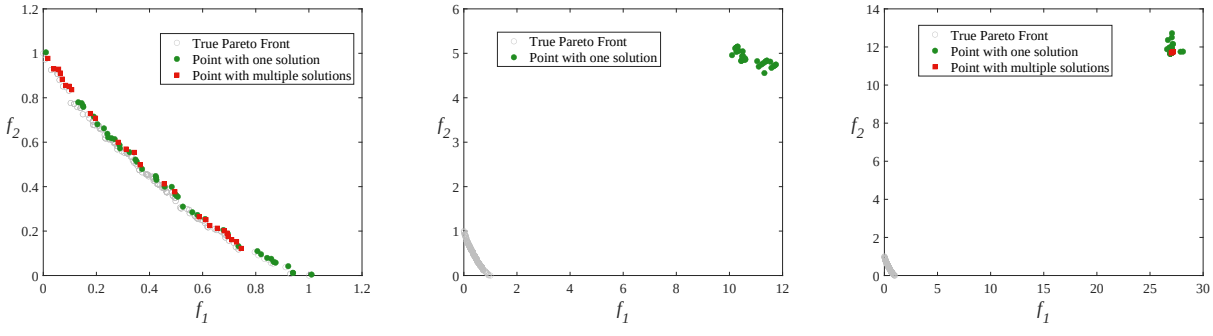

(a) TSPXEA (b) DNEA-TSP (c) EAG

(d) DCDG (e) DYN (f) NMA

Fig. S.7. The solution set of a single run in the objective space obtained by each compared algorithm on lin105+D1. This particular run is associated with the result closest to the mean IGDM value. (a) TSPXEA. (b) DNEA-TSP. (c) EAG. (d) DCDG. (e) DYN. (f) NMA.

S-VI. The convergence plots towards true Pareto fronts

Figs. S.8-S.11 show the average IGDM, HV, and GD values over 30 runs with regard to the number of evaluated solutions obtained by the compared algorithms on uni1+D1, bays29+D1, att48+D1, and lin105+D1, respectively. The scales of the test problems increase gradually.

We can see from Fig. S.8 that all the compared algorithms converge quickly on this easy test problem regarding three indicators. One exception is NMA. Its IGDM and HV values become worse as the number of evaluated solutions increases. However, its GD delines more quickly than the other algorithms. The reason is that NMA deletes many solutions that are not well-converged in its archive, which results in a loss of diversity.

We have the following observations from Figs. S.9-S.11. (1) TSPXEA converges most quickly regarding three indicators on these test problems, followed by DCDG. (2) The other algorithms converge slowly, especially when the scale of the problem is large. (3) The IGDM values of NMA on att48+D1 and those of DNEA-TSP, EAG, DYN, and NMA on lin105+D1 are always 1. Also, the HV values of NMA on att48+D1 and those of DNEA-TSP, EAG, DYN, and NMA on lin105+D1 are always 0. That is because of their poor convergence performance.

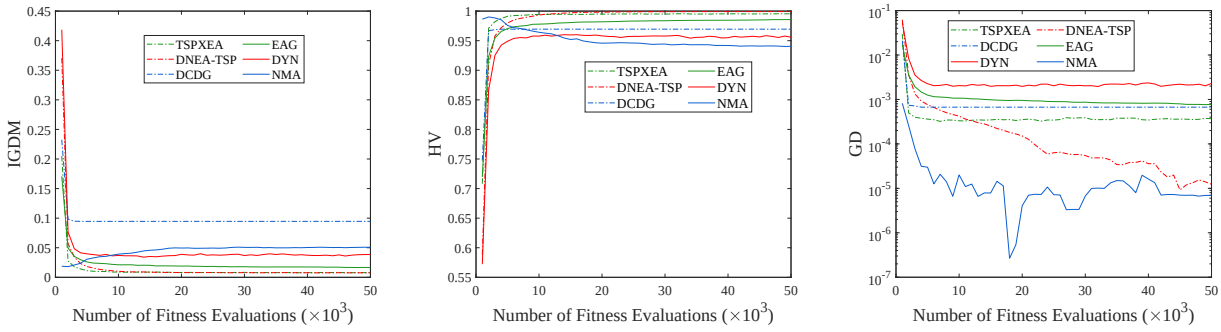

(a) (b) (c)

Fig. S.8. The average IGDM, HV, and GD values over 30 runs with regard to the number of evaluated solutions obtained by the compared algorithms on uni1+D1.

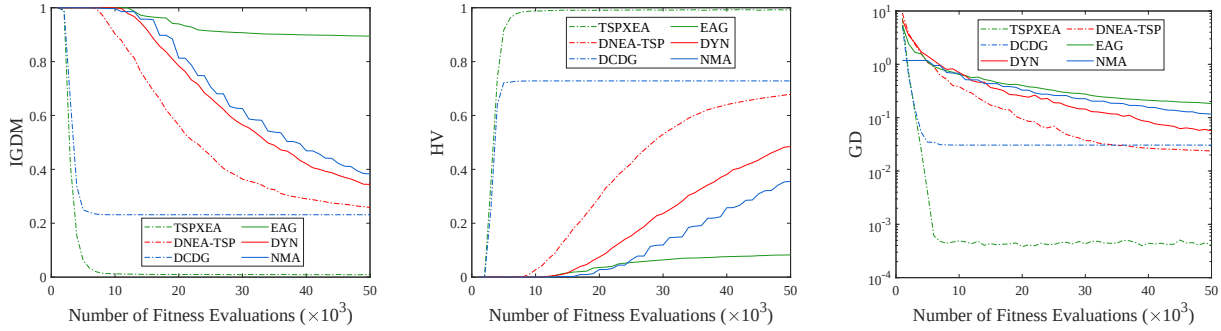

(a) (b) (c)

Fig. S.9. The average IGDM, HV, and GD values over 30 runs with regard to the number of evaluated solutions obtained by the compared algorithms on bays29+D1.

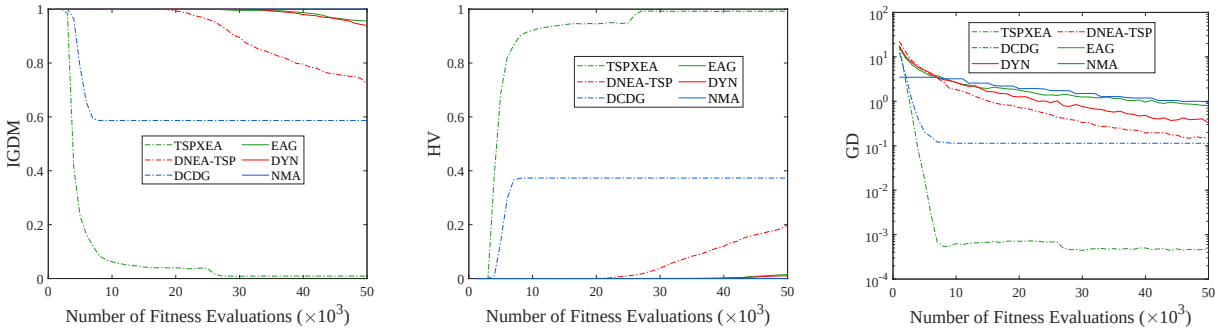

(a) (b) (c)

Fig. S.10. The average IGDM, HV, and GD values over 30 runs with regard to the number of evaluated solutions obtained by the compared algorithms on att48+D1.

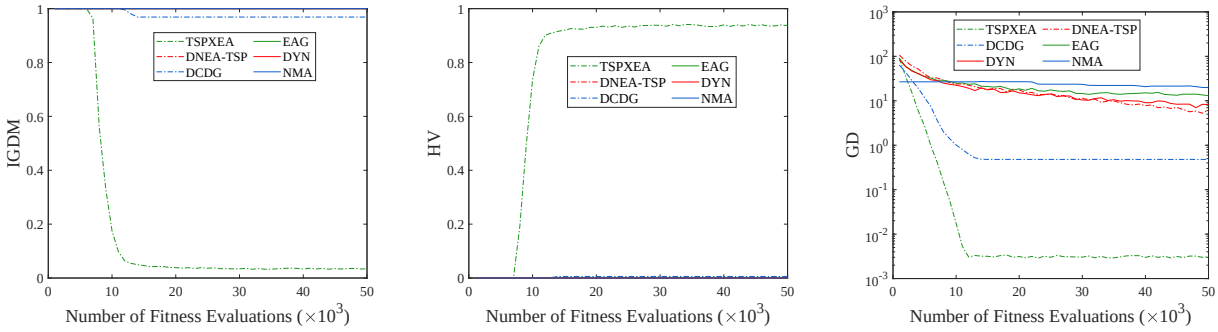

(a) (b) (c)

Fig. S.11. The average IGDM, HV, and GD values over 30 runs with regard to the number of evaluated solutions obtained by the compared algorithms on lin105+D1.

S-VII. Why the GD values obtained by TSPXEA are not always the best on small-scale problems

As we can observe from Table S.XIV that the GD values obtained by TSPXEA are not always the best on small-scale problems (i.e., the 'uni1' series).

One is that some solutions obtained by TSPXEA are not very close to the Pareto front. This is because TSPXEA always tries to maintain good diversity in both the objective and decision space. We have such an observation in Fig. S.4. In contrast, the solutions obtained by some compared algorithms (e.g., DCDG and NMA) are very close to the Pareto front since they can concentrate on the search in the objective space. Since GD is the average distance of all non-dominated solutions to the Pareto front, the GD values obtained by TSPXEA are larger than those by DCDG and NMA.

The other reason is that the search area in the decision space covered by EAX-ND is smaller than other genetic operators. This is because EAX-ND is designed to efficiently find good solutions under a limited computation time by focusing the search on only promising regions. When huge computing resources (i.e., a large number of fitness evaluations) are used to solve small-scale problems, other genetic operators have a higher chance to find the Pareto optimal solutions than EXA-ND does. Assume that we use a 'genetic' operator which randomly generates solutions. Such an operator can cover the entire search space. We can certainly find the Pareto optimal solutions by this operator if we have adequate computing resources. Fig. S.12 shows the number of different solutions with regard to the number of fitness evaluations generated by each algorithm on uni1+D1. Note that the number of different solutions obtained by NMA is from only one weight vector. The number of different solutions from 100 weight vectors would be 100 times as much as this. We can see from Fig. S.12 that the number of different solutions generated by TSPXEA is smaller than those of the other algorithms except for DCDG. DCDG uses a local search operator. Because the diversity of solutions obtained by DCDG is poor on small-scale problems, the local search operator can only search for a small region defined by neighborhood. The search behavior of EAX-ND in TSPXEA is guided by some 'preference.' The 'preference' is given by non-dominated ranking and finding the minimum value of f^C in (6). This is why TSPXEA generates fewer different solutions. However, such a 'preference' can help TSPXEA to converge quickly on large-scale problems.

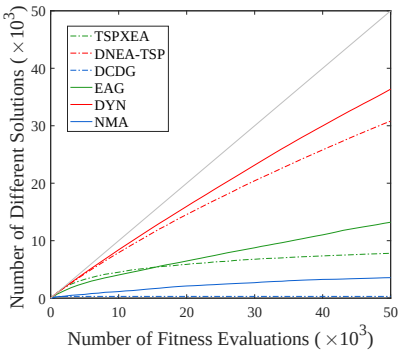

Fig. S.12. The number of different solutions with regard to the number of fitness evaluations generated by each algorithm on uni1+D1.

S-VIII. What an Unlimited Archive Can Do for MMTSPs

In this section, we modify typical multiobjective TSP algorithms (i.e., DCDG and EGA) by adding an archive of an unlimited size that collects all the non-dominated solutions during the evolutionary process. The modified DCDG and EGA are denoted as DCDG-archive and EAG-archive. We want to observe whether they can obtain equivalent Pareto optimal solutions with such a modification. We also create TSPXEA-archive in the same way to investigate the effect of the archive on TSPXEA. We apply these algorithms to uni1+D1, bays29+D1, att48+D1, and lin105+D1. The stop criterion is the number of evaluated solutions reaches $50,000$. Please note that the time and space complexity of such an archive is extremely high, which is unfair to the other compared algorithms. Thus, we do not include the algorithms with archives in the experiments in Subsection V-D.

Tables S.III-S.V show the average IGDM, HV, and GD values over 30 runs and the corresponding performance scores obtained by TSPXEA, DCDG, and EGA, and their respective archive versions on uni1+D1, bays29+D1, att48+D1, and lin105+D1. We can see from these tables that the algorithms with archives perform generally better than their original versions according to the three indicators. Therefore, the archive can improve the performance of an algorithm, especially the diversity performance. On the other hand, the original TSPXEA even outperforms DCDG-archive and EAG-archive, which in turn verifies the superiority of the proposed TSPXEA.

TABLE S.III
THE AVERAGE IGDM VALUES OVER 30 RUNS AND THE CORRESPONDING PERFORMANCE SCORES OBTAINED BY SIX ALGORITHMS.

IGDM	TSPXEA		DCDG		EAG		TSPXEA-archive		DCDG-archive		EAG-archive	
uni1+D1	7.640E-3	3	9.460E-2	0	1.660E-2	1	1.359E-3	5	1.389E-2	2	9.763E-3	3
bays29+D1	7.847E-3	4	2.316E-1	2	8.944E-1	0	2.203E-4	5	2.196E-1	2	6.869E-1	0
att48+D1	8.267E-3	4	5.868E-1	2	9.537E-1	0	8.627E-4	5	5.835E-1	2	9.935E-1	0
lin105+D1	2.309E-2	4	9.687E-1	2	1.000E+0	0	1.700E-2	4	9.687E-1	2	1.000E+0	0
APS	3.75		1.5		0.25		4.75		2		0.75	

TABLE S.IV
THE AVERAGE HV VALUES OVER 30 RUNS AND THE CORRESPONDING PERFORMANCE SCORES OBTAINED BY SIX ALGORITHMS.

HV	TSPXEA		DCDG		EAG		TSPXEA-archive		DCDG-archive		EAG-archive	
uni1+D1	9.952E-1	3	9.695E-1	0	9.856E-1	1	9.989E-1	5	9.968E-1	4	9.895E-1	1
bays29+D1	9.952E-1	4	7.284E-1	2	8.269E-2	0	1.000E+0	5	7.331E-1	2	2.439E-1	1
att48+D1	9.942E-1	4	3.730E-1	2	1.583E-2	0	9.991E-1	5	3.750E-1	2	8.119E-4	0
lin105+D1	9.616E-1	4	5.790E-3	2	0.000E+0	0	9.670E-1	4	5.790E-3	2	0.000E+0	0
APS	3.75		1.5		0.25		4.75		2.5		0.5	

TABLE S.V
THE AVERAGE GD VALUES OVER 30 RUNS AND THE CORRESPONDING PERFORMANCE SCORES OBTAINED BY SIX ALGORITHMS.

GD	TSPXEA		DCDG		EAG		TSPXEA-archive		DCDG-archive		EAG-archive	
uni1+D1	3.584E-4	3	6.708E-4	0	7.827E-4	0	9.760E-5	5	2.633E-4	4	5.516E-4	1
bays29+D1	3.102E-4	4	3.059E-2	2	1.825E-1	0	0.000E+0	5	1.804E-2	2	2.123E-1	0
att48+D1	4.492E-4	4	1.138E-1	2	7.887E-1	1	9.511E-5	5	7.683E-2	3	1.048E+0	0
lin105+D1	1.940E-3	4	4.796E-1	2	1.318E+1	0	1.085E-3	5	4.673E-1	2	1.211E+1	0
APS	3.75		1.5		0.25		5		2.75		0.25	

Fig. S.13 shows the solution sets of a single run in the objective space obtained by TSPXEA-archive, DCDG-archive, and EAG-archive on uni1+D1. This particular run is associated with the result closest to the mean IGDM value. Compared to the results in Fig. S.13, we have the following observations: (1) The archive does help the typical multiobjective TSP algorithms (such as DCDG and EAG) to find points with multiple solutions. (2) The archive can help TSPXEA to identify more multiple equivalent solutions. (3) TSPXEA-archive is obviously considered better than DCDG-archive and EAG-archive in searching for equivalent Pareto optimal solutions. The reason for the first two observations is that the number of the Pareto optimal solutions to an MMTSP is finite (Please refer to Table I in the paper). Thus, the archive may collect equivalent Pareto optimal solutions during the evolutionary process. For a continuous MMOP whose number of Pareto optimal solutions is infinite or a combinatorial MMOP whose number of Pareto optimal solutions is numerous, such an archive may be proven ineffective in maintaining a large number of equivalent Pareto optimal solutions since multiple equivalent solutions are usually not examined by standard evolutionary multiobjective optimization algorithms.

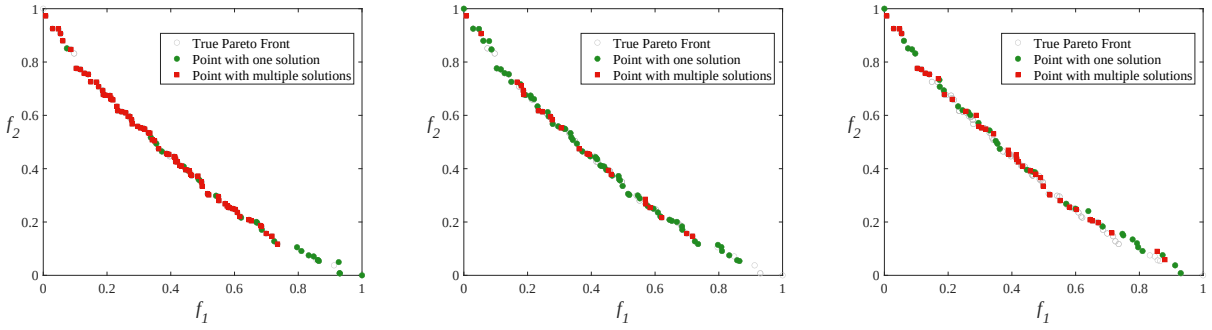

Fig. S.13. The solution set of a single run in the objective space obtained by each compared algorithm on uni1+D1. This particular run is associated with the result closest to the mean IGDM value. (a) TSPXEA-archive. (b) DCDG-archive. (c) EAG-archive.

S-IX. The Characteristics of the Test Problems

This section discusses the characteristics of the test problems generated by our test problem generator.

Fig. S.14 shows some randomly generated solutions and the true Pareto fronts of att48+D1 and att48+D3. The gray circles around the left-bottom corner are the Pareto optimal solutions (i.e., the true Pareto front). The red circles are randomly generated solutions. For each Pareto optimal solution, the sub-tour in the D-type vertices (i.e., the bold gray lines in Fig. S.15(a)) is fixed, and the other part of the tour (from d_1 to d_2 through the C-type vertices, i.e., the bold red lines in Fig. S.15(a)) is randomly re-generated. The resulting solutions are shown by the blue circles in Fig. S.14. Similarly, we obtain solutions shown by the green circles in Fig. S.14, where only the sub-tour in the C-type vertices is randomly re-generated (i.e., the bold red lines in Fig. S.15(b)). That is, green circle solutions contain edges (c_1, d_1) and (c_2, d_2) while blue circle solutions usually do not.

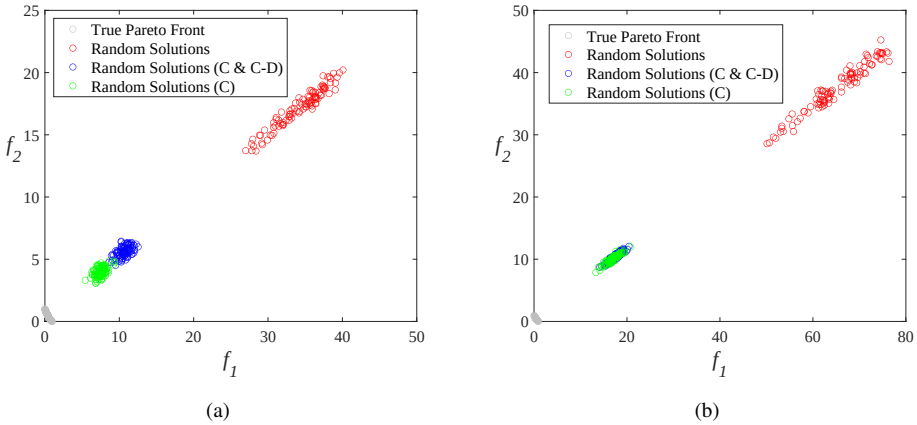

Fig. S.14. The random solutions (red, blue, green) and the true Pareto front (gray). (a) att48+D1. (b) att48+D3.

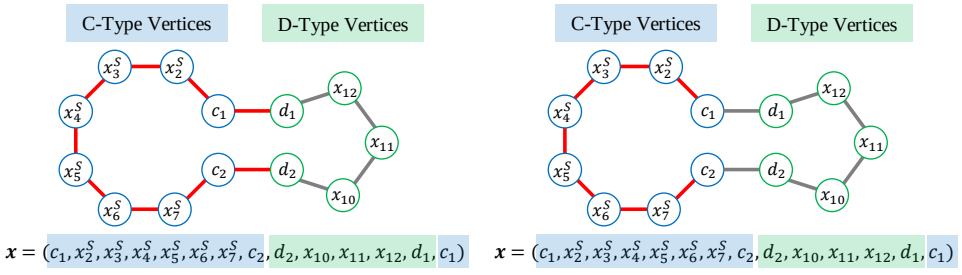

Fig. S.15. Assume we have a Pareto optimal solution shown in Fig. 6 (i.e., a gary circle solution in Fig. S.14). (a) To obtain a blue circle solution in Fig. S.14, we fix the sub-tour in the D-type vertices (i.e., the bold gray lines) and randomly re-generate the other part of the tour (from d_1 to d_2 through the C-type vertices, i.e., the bold red lines). (b) Similarly, we obtain a green circle solution in Fig. S.14, where only the sub-tour in the C-type vertices is randomly re-generated (i.e., the bold red lines).

We have the following observations from Fig. S.14, which indicate the characteristics of the test problems. (1) The random solutions (i.e., red circles) are far away from the Pareto front. This is the same as the following property of the standard single-objective TSP: Randomly generated solutions are usually far away from the optimal solution. Since the search for the optimal tour in the C-type vertices is a single-objective TSP, our test problems have the same property as the standard TSP. In such a case, an algorithm is required to have a strong ability to converge from a randomly initialized population (i.e., red circles) and the true Pareto front. (2) All solutions are around a single line in each figure in Fig. S.14. This means that the two objectives are heavily correlated (i.e., the conflict between the two objectives is not strong). This is because the edges among the C-type vertices have no conflict (and the number of the C-type vertices is large in our test problems). However, the two objectives are clearly inconsistent with each other around the Pareto front as shown by the gray circles. (3) If compared with the large distance between the true Pareto front (i.e., gray circles) and the randomly generated solutions (i.e., red circles), the distance between the green solutions and the blue solutions in Fig. S.14(a) is small. In Fig. S.14(b), they are almost overlapping. The difference between these two solution sets is whether two edges (c_1, d_1) and (c_2, d_2) are included (in the green solutions) or not (in the blue solutions). This observation suggests that these two edges do not have any dominant effect on the solution quality, whereas they are always included in the Pareto optimal solutions. Similar observations are also obtained from the other test problems with a large number of C-type vertices.

Now let us generate some new test problems with no C-type vertices (i.e., by setting $k^C = 0$), but a large number of D-type vertices. First, we generate three test problems with 20, 50, and 100 D-type vertices, denoted as R-20-M, R-50-M, and R-100-M, respectively. Then, without creating multimodality (i.e., without implementing lines 14-21 in Algorithm 1), in a similar way, we generate three more test problems, denoted as R-20-T, R-50-T, and R-100-T. These problems are regarded as traditional multi-objective TSPs. We may consider these six problems are more 'general' since they look more 'random' with no C-type vertices. We call them the 'R' series (i.e., random). It is computationally intractable to identify the true Pareto optimal solutions to each of these six problems. The equivalent Pareto optimal solutions are also unknown.

Fig. S.16 shows the random solutions (red circles) and the solutions obtained by TSPXEA (blue circles) on R-50-M and R-100-M. Since we do not know the true Pareto front, we use the solutions obtained by TSPXEA as an approximate Pareto front.

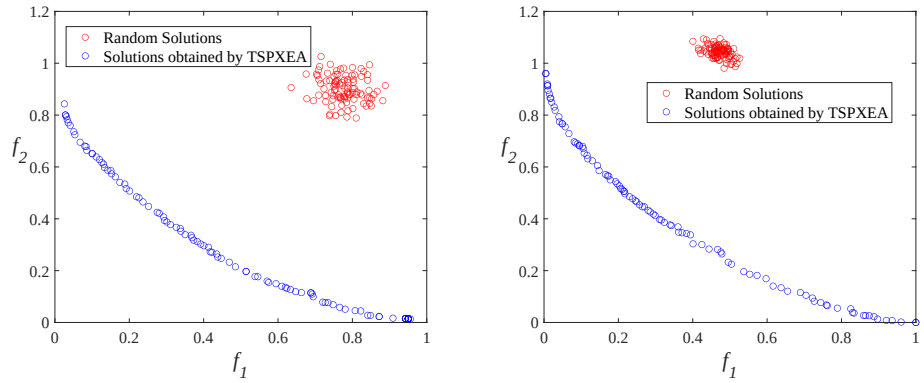

Fig. S.16. The random solutions (red circles) and the solutions obtained by TSPXEA (blue circles). (a) R-50-M. (b) R-100-M.

We can see from Fig. S.16 that the random solutions (red circles) locates in a relatively small region and are close to the approximate Pareto front (blue circles) (compared to those in Fig. S.14). The approximate Pareto front has a much wider spread than the random solutions. The reason for this observation is that the conflict between the objectives is strong. In such a case, an algorithm is required to have a strong diversification ability of the population. In contrast, the ability to converge is not emphasized. Similar observations are also obtained from those of the 'R' series.

The characteristics of the test problems with the C-type vertices (e.g., att48+D1 and att48+D3) and without the C-type vertices (e.g., 'R' series) are different as explained by the abovementioned observations. However, we cannot say which kind of problem is more general in practice. Real-world multiobjective TSPs may have either weak or strong conflict among objectives. For instance, the travel time (the first objective) is usually, but not always, directly proportional to the ticket price (the second objective). The real-world example in Fig. 3 in Subsection II-C is such a case. The distribution of its solutions in Fig. 3 looks similar to that in Fig. S.14. However, we may have different cases. For example, in a special delivery problem, a large benefit of delivering cargos (the first objective) may correspond to high risk (the second objective). Then, such a problem is likely a test problem of the 'R' series.

Our test problem generator provides a novel way to generate large-scale MMTSPs (as well as traditional multi-objective TSPs) with known Pareto optimal solutions. However, in order to identify all true Pareto optimal solutions, the number of D-type vertices cannot be large (whereas the number of C-type vertices can be large). As a result, the conflict among objectives is usually not strong.

S-X. The results on the 'R' series

In this section, we compare TSPXEA with the other algorithms on the 'R' series test problems. The parameter settings of the algorithms are the same as those in Section V in the paper. Because we do not know the true Pareto optimal solutions to these problems, indicators such as IGDM and GD cannot be applied. We evaluate the performance of a solution set obtained by an algorithm in the following three ways.

(i) HV: Table S.VI shows the average HV values over 30 runs and the corresponding performance scores obtained by the compared algorithms. Note that we normalize the objective space of each test problem so that the estimated ideal and nadir points from the non-dominated front obtained by all algorithms are $(0, 0)$ and $(1, 1)$, respectively. Then, the reference point for HV calculation is specified as $(1.1, 1.1)$.

TABLE S.VI
THE AVERAGE HV VALUES OVER 30 RUNS AND THE CORRESPONDING PERFORMANCE SCORES OBTAINED BY THE COMPARED ALGORITHMS (5: BEST, 0: WORST).

HV	TSPXEA		DNEA-TSP		DCDG		EAG		NMA		DYN	
R-20-T	9.152E-1	5	8.709E-1	2	8.822E-1	3	4.356E-1	0	9.114E-1	4	7.082E-1	1
R-20-M	8.488E-1	4	8.213E-1	2	8.337E-1	3	4.156E-1	0	8.514E-1	5	7.077E-1	1
R-50-T	9.921E-1	5	7.140E-1	2	9.800E-1	4	1.589E-1	0	7.230E-1	3	4.417E-1	1
R-50-M	9.194E-1	4	6.994E-1	3	9.190E-1	4	1.648E-1	0	6.872E-1	2	5.358E-1	1
R-100-T	1.075E+0	5	8.163E-1	2	1.063E+0	4	7.937E-1	1	8.914E-1	3	3.197E-1	0
R-100-M	9.118E-1	4	8.060E-1	3	9.233E-1	5	7.858E-1	1	7.988E-1	2	5.940E-1	0
APS	4.5		2.3		3.8		0.3		3.2		0.7	

We have the following observations from Table S.VI: (1) The HV values obtained by TSPXEA are the best among the compared algorithms on average. (2) DCDG performs well on large-scale problems (those with 50 and 100 vertices). (3) NMA shows good performance on small-scale problems (those with 20 vertices). It should be noted that the computational cost of NMA is 100 times larger than those of the other algorithms. (4) The average HV value of TSPXEA on R-20-M is slightly smaller than that of NMA, and the average HV value of TSPXEA on R-100-M is slightly smaller than that of DCDG. The reason for such a slightly inferior performance on some test problems is that TSPXEA tries to promote diversity in both the objective and decision spaces, whereas HV only evaluates the performance in the objective space. Maintaining equivalent solutions may slightly degrade the diversity in the objective space.

(ii) Multimodality Ratio (MR): MR is the ratio of solutions with the same objective vector and different decision variable vectors in an obtained solution set.[1] Table S.VII shows the average MR values over 30 runs and the corresponding performance scores obtained by the compared algorithms.

[1]For example, assume that we have the following solution set that consists of 10 different solutions: $\{\boldsymbol{x}_1, \ldots, \boldsymbol{x}_{10}\}$. $\boldsymbol{f}(\boldsymbol{x}_1) = \cdots = \boldsymbol{f}(\boldsymbol{x}_5)$, $\boldsymbol{f}(\boldsymbol{x}_5) \neq \boldsymbol{f}(\boldsymbol{x}_6)$, $\boldsymbol{f}(\boldsymbol{x}_6) = \boldsymbol{f}(\boldsymbol{x}_7)$, and $\boldsymbol{f}(\boldsymbol{x}_8)$, $\boldsymbol{f}(\boldsymbol{x}_9)$, and $\boldsymbol{f}(\boldsymbol{x}_{10})$ are different from any other objective vector. In this case, MR is calculated as $(5+2)/10 = 0.7$ since $(5+2)$ solutions show multimodality. If some solutions are the same in the decision space (i.e., if some solutions are duplicates), those solutions are counted as a single solution. For example, if $\boldsymbol{x}_1 = \boldsymbol{x}_2 = \boldsymbol{x}_3$ in the above example, MR is calculated as $(3+2)/10$ since $\boldsymbol{x}_1$, $\boldsymbol{x}_2$, and $\boldsymbol{x}_3$ are counted as a single solution in the numerator of the MR calculation.

TABLE S.VII
THE AVERAGE MR VALUES OVER 30 RUNS AND THE CORRESPONDING PERFORMANCE SCORES OBTAINED BY THE COMPARED ALGORITHMS (5: BEST, 0: WORST).

MR	TSPXEA		DNEA-TSP		DCDG		EAG		NMA		DYN	
R-20-T	0.000E+0	0	0.000E+0	0	0.000E+0	0	0.000E+0	0	0.000E+0	0	0.000E+0	0
R-20-M	2.473E-1	5	4.000E-3	1	0.000E+0	0	7.337E-3	1	2.112E-1	4	2.965E-3	1
R-50-T	0.000E+0	0	0.000E+0	0	0.000E+0	0	0.000E+0	0	0.000E+0	0	0.000E+0	0
R-50-M	2.223E-1	4	4.316E-1	5	0.000E+0	0	9.981E-2	3	1.024E-3	0	3.119E-2	2
R-100-T	0.000E+0	0	0.000E+0	0	0.000E+0	0	0.000E+0	0	0.000E+0	0	0.000E+0	0
R-100-M	1.270E-1	5	6.667E-4	0	0.000E+0	0	2.468E-2	3	1.322E-3	0	4.450E-2	4
APS	2.3		1.0		0.0		1.2		0.7		1.2	

We can see from Table S.VII that no algorithm finds different solutions with the same objective vector to the three 'traditional' problems as expected. The MR values obtained by TSPXEA are larger on the multimodal problems. The MR of DNEA-TSP is large on R-50-M. However, the solution set obtained by DNEA-TSP is not well converged according to the results of HV in Table S.VI. EGA, NMA, and DYN may find solutions with the same objective vector on some problems. DCDG finds no such solutions to all the problems.

(iii) Visualization of the solution sets: Figs. S.17-S.22 show the solution set of a single run in the objective space obtained by each compared algorithm on R-20-T, R-20-M, R-50-T, R-50-M, R-100-T and R-100-M, respectively, where a green circle represents a point corresponding to a single solution while a red square indicates a point corresponding to multiple solutions (i.e., different solutions in the decision space whereas they are equivalent in the objective space). A single run with the closest HV result to the mean HV value is selected for visualization from 30 runs of each algorithm on each test problem.

We can see from these figures that the solutions obtained by TSPXEA converge and spread well in the objective space on all test problems. TSPXEA can also find some points with multiple solutions to multimodal problems. DNEA-TSP has an acceptable convergence performance. However, it fails to promote diversity in the objective space. DCDG converges well on all test problems. However, it encounters diversity issues on small-scale problems. Besides, it finds no solutions with the multimodal property (no different solutions with the same objective vector). NMA performs well on small-scale problems but fails to approximate the Pareto front on large-scale problems. EAG and DYN experience convergence issues on all test problems.

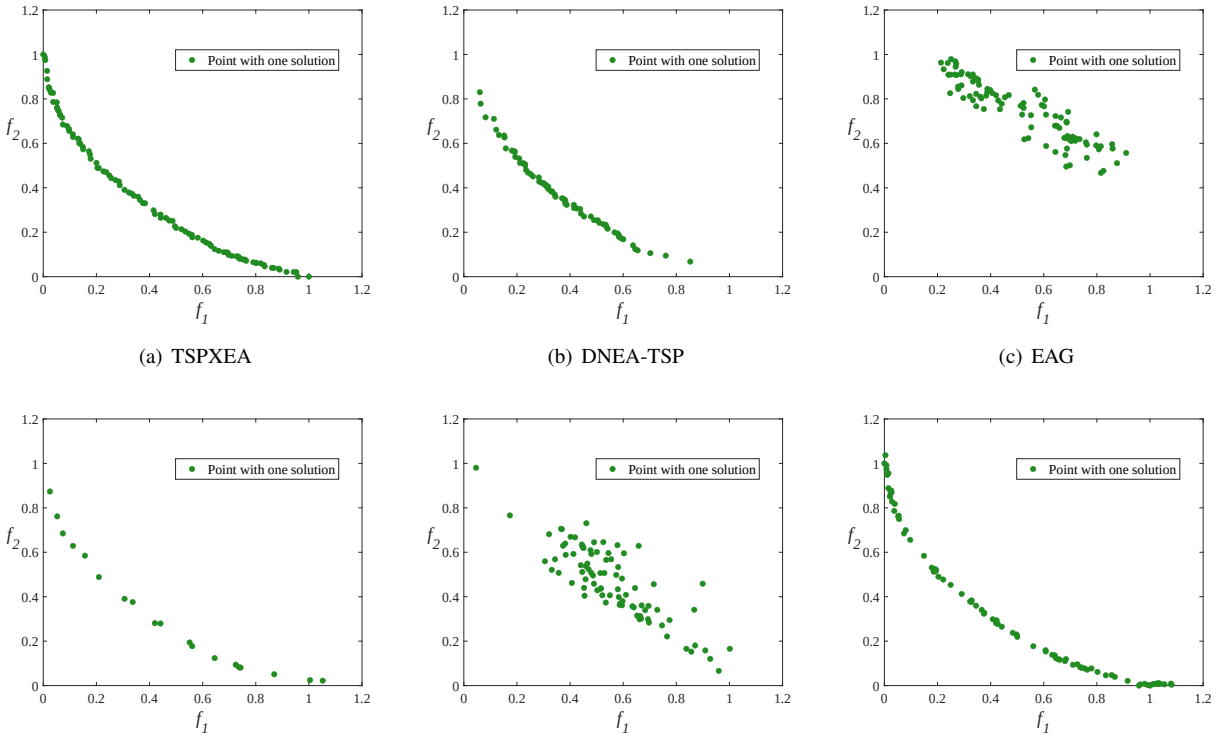

(a) TSPXEA (b) DNEA-TSP (c) EAG

(d) DCDG (e) DYN (f) NMA

Fig. S.17. The solution set of a single run in the objective space obtained by each compared algorithm on R-20-T. This particular run is associated with the result closest to the mean HV value. (a) TSPXEA. (b) DNEA-TSP. (c) EAG. (d) DCDG. (e) DYN. (f) NMA.

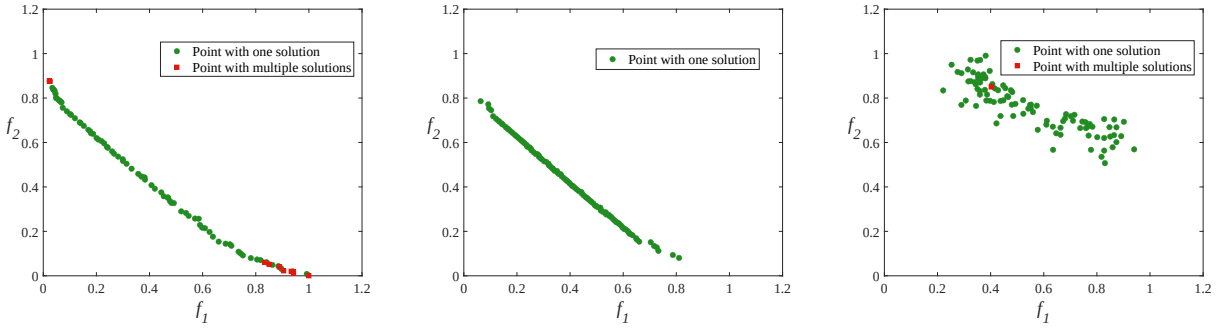

(a) TSPXEA (b) DNEA-TSP (c) EAG

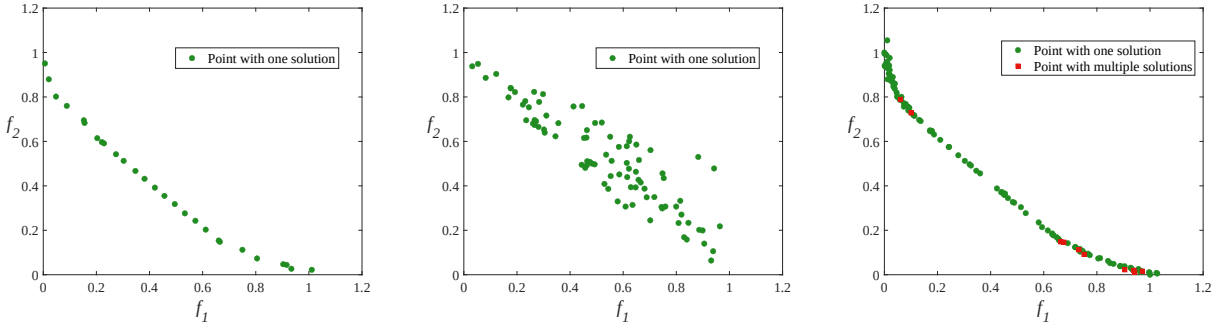

(d) DCDG (e) DYN (f) NMA

Fig. S.18. The solution set of a single run in the objective space obtained by each compared algorithm on R-20-M. This particular run is associated with the result closest to the mean HV value. (a) TSPXEA. (b) DNEA-TSP. (c) EAG. (d) DCDG. (e) DYN. (f) NMA.

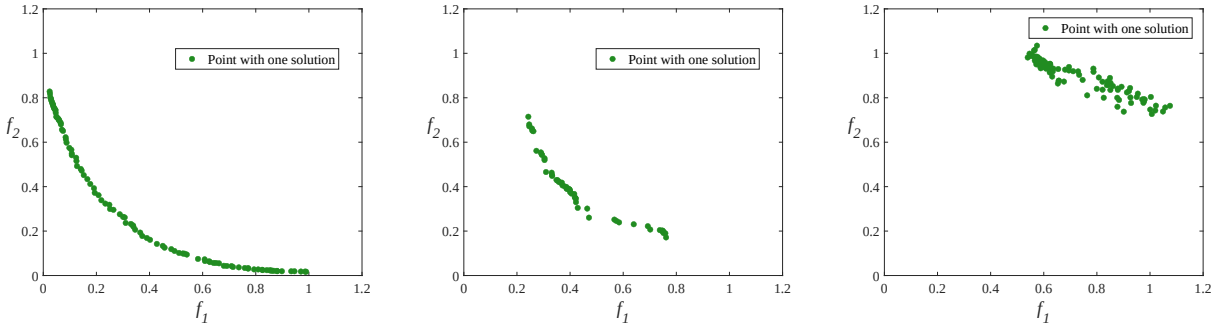

(a) TSPXEA (b) DNEA-TSP (c) EAG

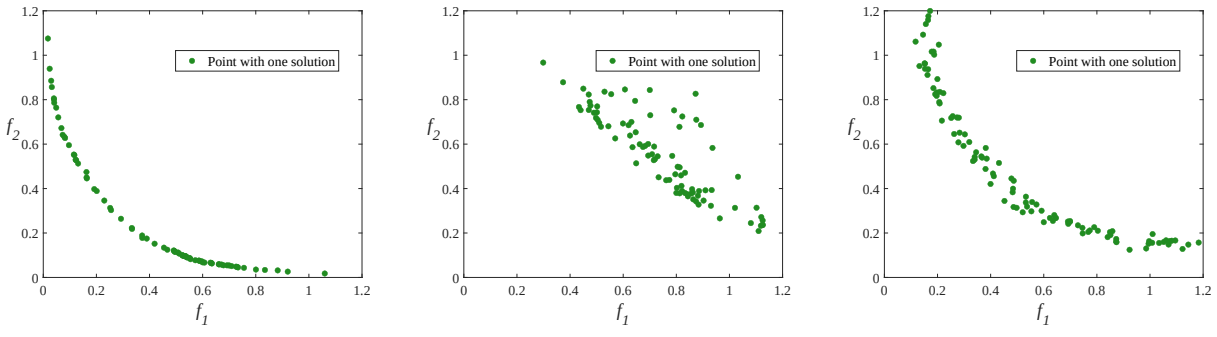

(d) DCDG (e) DYN (f) NMA

Fig. S.19. The solution set of a single run in the objective space obtained by each compared algorithm on R-50-T. This particular run is associated with the result closest to the mean HV value. (a) TSPXEA. (b) DNEA-TSP. (c) EAG. (d) DCDG. (e) DYN. (f) NMA.

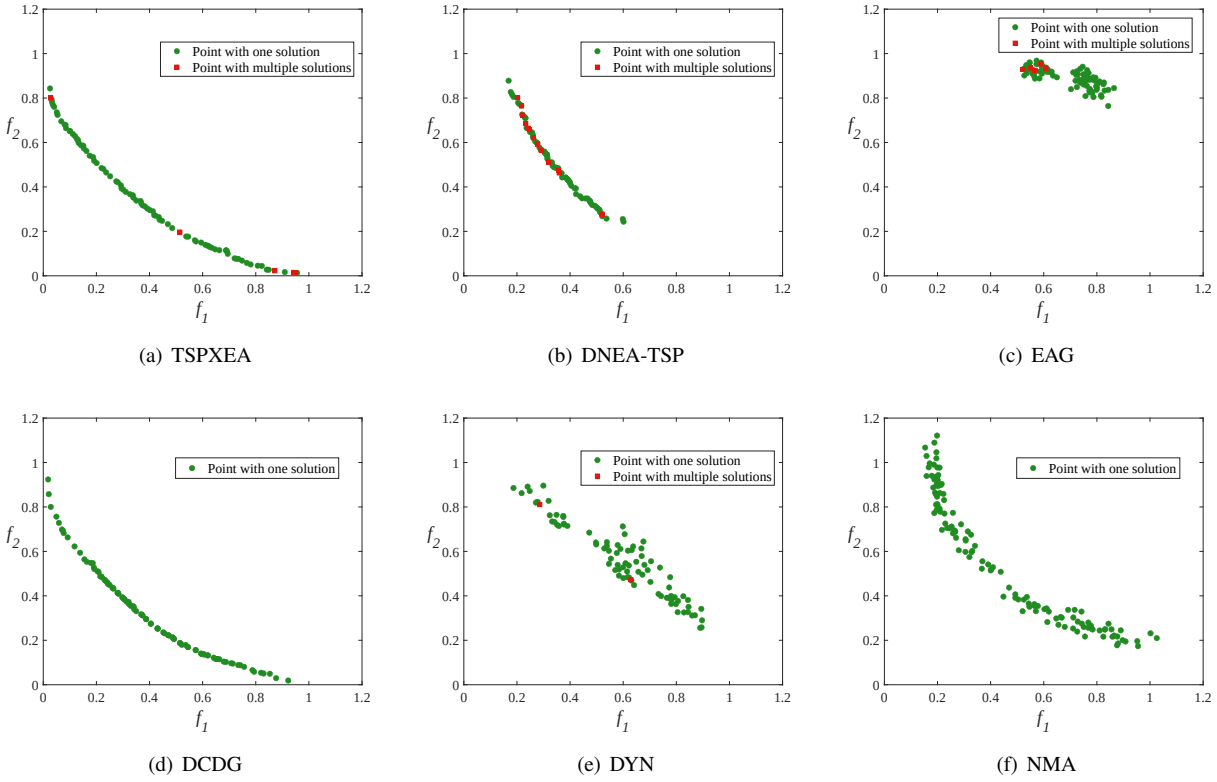

(a) TSPXEA (b) DNEA-TSP (c) EAG

(d) DCDG (e) DYN (f) NMA

Fig. S.20. The solution set of a single run in the objective space obtained by each compared algorithm on R-50-M. This particular run is associated with the result closest to the mean HV value. (a) TSPXEA. (b) DNEA-TSP. (c) EAG. (d) DCDG. (e) DYN. (f) NMA.

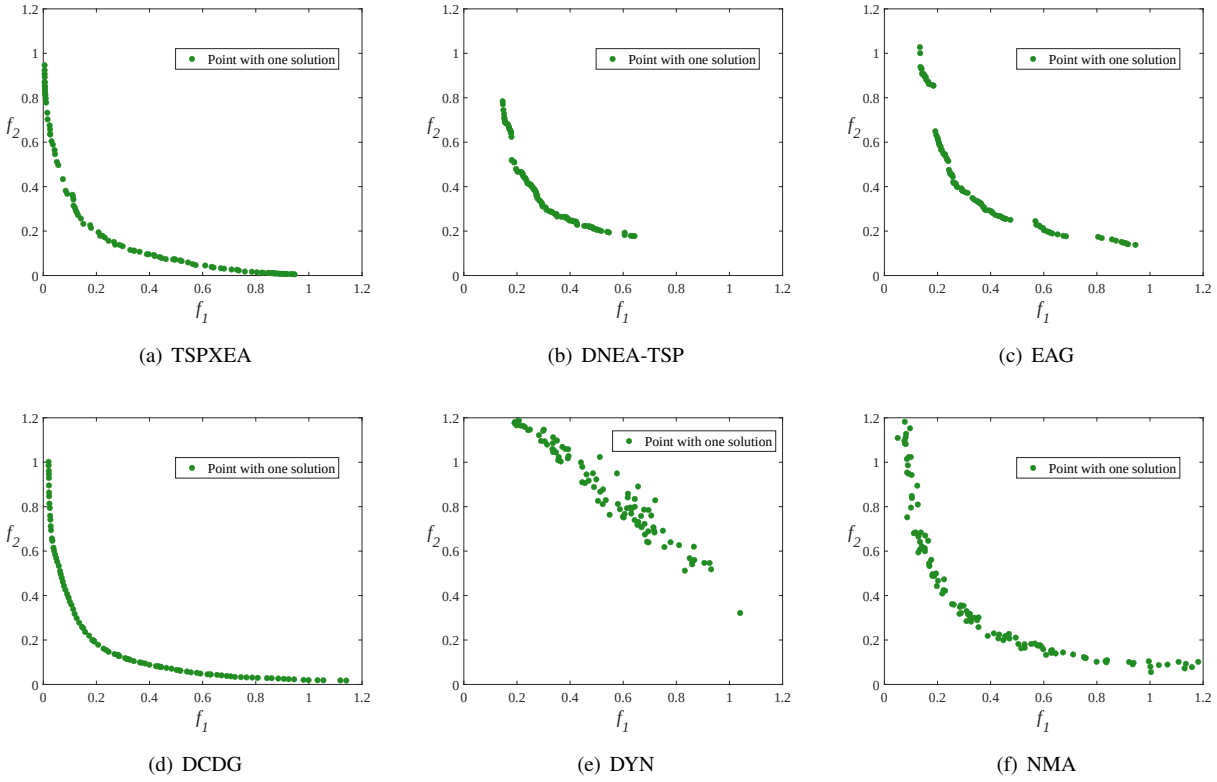

(a) TSPXEA (b) DNEA-TSP (c) EAG

(d) DCDG (e) DYN (f) NMA

Fig. S.21. The solution set of a single run in the objective space obtained by each compared algorithm on R-100-T. This particular run is associated with the result closest to the mean HV value. (a) TSPXEA. (b) DNEA-TSP. (c) EAG. (d) DCDG. (e) DYN. (f) NMA.

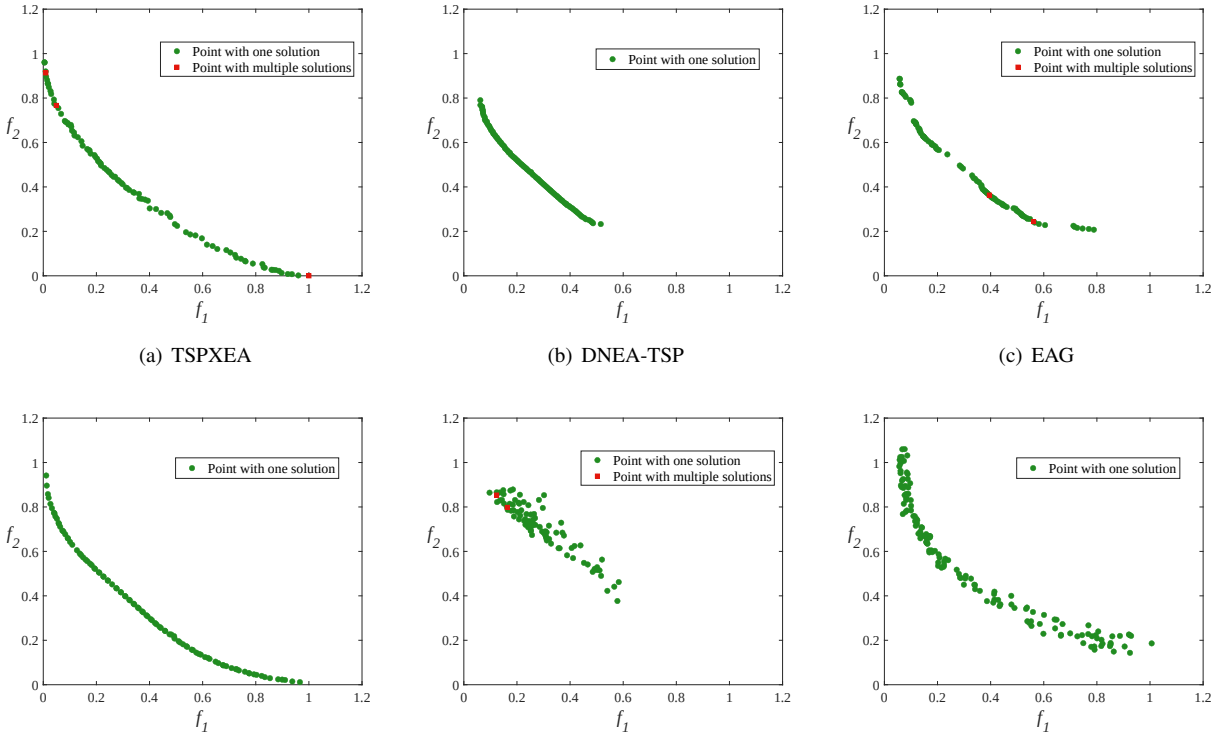

(a) TSPXEA (b) DNEA-TSP (c) EAG

(d) DCDG (e) DYN (f) NMA

Fig. S.22. The solution set of a single run in the objective space obtained by each compared algorithm on R-100-M. This particular run is associated with the result closest to the mean HV value. (a) TSPXEA. (b) DNEA-TSP. (c) EAG. (d) DCDG. (e) DYN. (f) NMA.

S-XI. The performance of TSPXEA on multimodal single-objective TSPs

In this section, we investigate the performance of TSPXEA on multimodal single-objective TSPs. Although the proposed TSPXEA is not designed to solve such problems, we can apply TSPXEA in the following manner. First, we transform the single-objective TSP into a multiobjective TSP with two objectives. The two objectives of the generated multiobjective TSP are the same as the objective in the single-objective TSP. Then, we use TSPXEA to solve the multiobjective TSP.

We use MSTSP1-25 [1] as test problems. In addition, we use the first objective of uni1+D5, bays+D5, and att48+D5 as three additional test problems. These three problems are still denoted as uni1+D5, bays29+D5, and att48+D5. We also use gr24 and gr48 from TSPLIB as test problems. The scale (i.e., the number of vertices, denoted as n) of each problem and the number of equivalent optimal solutions to each problem (denoted as n_o) are listed in Tables S.VIII and S.IX.

We apply two versions of TSPXEA to solve the test problems. One is TSPXEA-W which only uses EAX-W. The other is TSPXEA-ND which only uses EAX-ND. We compare them with NMA in solving these problems. NMA is considered a state-of-the-art algorithm for multimodal single-objective TSPs.

We use two indicators to evaluate the performance of the compared algorithms on the test problems. The first is the ratio of the obtained equivalent optimal solutions (RO), which is calculated as follows:

$$\text{RO} = \frac{n_a}{n_o}, \tag{S.8}$$

where n_a denotes the number of the equivalent optimal solutions obtained by the algorithm, and n_o is the number of the true equivalent optimal solutions in a test problem. For example, MSTSP1 has three equivalent optimal solutions. If an algorithm finds two of them, RO is calculated as $2/3$. RO is within the range of $[0, 1]$, and the larger, the better. The average value of RO is calculated over 30 runs of each algorithm on each test problem.

The other indicator is the diversity indicator (DI) which was used in the original study of NMA [1]. DI is calculated as

$$\text{DI} = \frac{\sum_{i=1}^{n_o} \max S(p_i, s_j)|_{j=1,\ldots,n_b}}{n \times n_o}, \tag{S.9}$$

where $p_i, i = 1, \ldots, n_o$ are the true equivalent optimal solutions to the test problem, $s_j, j = 1, \ldots, n_b$ refer to the solutions obtained by the algorithm, $S(p_i, s_j)$ is the number of common edges between solutions p_i and s_j (thus $0 \leq S(p_i, s_j) \leq n$), and n is the number of vertices/edges of the test problem. DI evaluates the similarity between the true optimal solutions and the obtained solutions in the decision space. DI is within the range of $[0, 1]$, and the larger, the better.

Tables S.VIII and S.IX show the average values of RO and DI over 30 runs obtained by the compared algorithms. From these tables, we have the following observations: (1) NMA usually obtains better RO and DI values than TSPXEA-ND and TSPXEA-W on small-scale problems with a small number of optimal solutions such as MSTSP1-6, MSTSP10, and uni1+D5. (2) When the scale of the problem is large (i.e., $n \geq 15$) or the number of true optimal solutions is large (i.e., $n_o \geq 16$), TSPXEA-ND and TSPXEA-W show clearly better performance than NMA. (3) TSPXEA-ND outperforms TSPXEA-W on the large-scale problems with many optimal solutions such as MSTSP16 and MSTSP18. When n is not less than 42, TSPXEA-ND performs better than TSPXEA-W, no matter how many optimal solutions there are.

TABLE S.VIII
THE RESULTS OF RO OBTAINED BY THE COMPARED ALGORITHMS ON MULTIMODAL SINGLE-OBJECTIVE OPTIMIZATION PROBLEMS.

Problem	n	n_o	TSPXEA-ND		TSPXEA-W		NMA	
MSTSP1	9	3	6.333E-1	0	6.111E-1	0	1.000E+0	2
MSTSP2	10	4	9.583E-1	0	9.833E-1	0	1.000E+0	1
MSTSP3	10	13	8.205E-1	0	7.974E-1	0	9.974E-1	2
MSTSP4	11	4	8.750E-1	0	8.083E-1	0	1.000E+0	2
MSTSP5	12	2	8.833E-1	0	7.833E-1	0	1.000E+0	2
MSTSP6	12	4	8.833E-1	1	7.417E-1	0	1.000E+0	2
MSTSP7	10	56	9.935E-1	1	9.929E-1	1	7.185E-1	0
MSTSP8	12	110	1.000E+0	1	1.000E+0	1	4.097E-1	0
MSTSP9	10	4	9.500E-1	0	9.917E-1	1	1.000E+0	1
MSTSP10	10	4	9.583E-1	0	9.333E-1	0	1.000E+0	2
MSTSP11	10	14	1.000E+0	0	1.000E+0	0	9.929E-1	0
MSTSP12	15	196	6.735E-1	1	6.735E-1	1	1.985E-1	0
MSTSP13	28	70	9.995E-1	1	1.000E+0	1	2.905E-1	0
MSTSP14	34	16	1.000E+0	1	9.500E-1	1	6.917E-1	0
MSTSP15	22	72	1.000E+0	1	1.000E+0	1	4.009E-1	0
MSTSP16	33	64	8.750E-1	2	7.396E-1	1	2.620E-1	0
MSTSP17	35	10	1.000E+0	1	9.600E-1	1	4.967E-1	0
MSTSP18	39	20	8.533E-1	2	6.133E-1	1	3.683E-1	0
MSTSP19	42	20	8.700E-1	2	6.400E-1	1	7.000E-2	0
MSTSP20	45	20	6.767E-1	1	5.567E-1	1	7.833E-2	0
MSTSP21	48	4	9.167E-1	2	6.000E-1	1	2.500E-2	0
MSTSP22	55	9	8.222E-1	2	5.259E-1	1	3.704E-3	0
MSTSP23	59	16	5.625E-1	2	3.208E-1	1	8.333E-3	0
MSTSP24	60	36	8.556E-1	2	5.204E-1	1	0.000E+0	0
MSTSP25	66	26	4.154E-1	1	3.769E-1	1	0.000E+0	0
uni1+D5	11	2	7.667E-1	0	6.500E-1	0	1.000E+0	2
bays29+D5	39	2	1.000E+0	1	9.000E-1	1	0.000E+0	0
att48+D5	58	2	1.000E+0	2	7.833E-1	1	0.000E+0	0
gr24	24	2	1.000E+0	1	1.000E+0	1	3.333E-2	0
gr48	48	2	1.000E+0	2	7.000E-1	1	0.000E+0	0
Average Performance Score			1.00		0.70		0.53	

TABLE S.IX
THE RESULTS OF DI OBTAINED BY THE COMPARED ALGORITHMS ON MULTIMODAL SINGLE-OBJECTIVE OPTIMIZATION PROBLEMS.

Problem	n	n_o	TSPXEA-ND		TSPXEA-W		NMA	
MSTSP1	9	3	9.185E-1	0	9.136E-1	0	1.000E+0	2
MSTSP2	10	4	9.917E-1	0	9.967E-1	0	1.000E+0	1
MSTSP3	10	13	9.641E-1	0	9.595E-1	0	9.995E-1	2
MSTSP4	11	4	9.773E-1	0	9.652E-1	0	1.000E+0	2
MSTSP5	12	2	9.806E-1	0	9.639E-1	0	1.000E+0	2
MSTSP6	12	4	9.806E-1	1	9.569E-1	0	1.000E+0	2
MSTSP7	10	56	9.987E-1	1	9.986E-1	1	9.409E-1	0
MSTSP8	12	110	1.000E+0	1	1.000E+0	1	8.911E-1	0
MSTSP9	10	4	9.900E-1	0	9.983E-1	1	1.000E+0	1
MSTSP10	10	4	9.917E-1	0	9.867E-1	0	1.000E+0	2
MSTSP11	10	14	1.000E+0	0	1.000E+0	0	9.986E-1	0
MSTSP12	15	196	9.565E-1	1	9.565E-1	1	8.662E-1	0
MSTSP13	28	70	1.000E+0	1	1.000E+0	1	9.254E-1	0
MSTSP14	34	16	1.000E+0	1	9.971E-1	1	9.808E-1	0
MSTSP15	22	72	1.000E+0	1	1.000E+0	1	9.360E-1	0
MSTSP16	33	64	9.924E-1	2	9.703E-1	1	9.295E-1	0
MSTSP17	35	10	1.000E+0	1	9.943E-1	1	9.560E-1	0
MSTSP18	39	20	9.827E-1	2	9.326E-1	0	9.383E-1	0
MSTSP19	42	20	9.839E-1	2	9.476E-1	1	8.644E-1	0
MSTSP20	45	20	9.639E-1	2	9.106E-1	0	8.820E-1	0
MSTSP21	48	4	9.818E-1	2	9.313E-1	1	8.470E-1	0
MSTSP22	55	9	9.798E-1	2	9.509E-1	1	8.005E-1	0
MSTSP23	59	16	9.452E-1	2	8.925E-1	1	8.269E-1	0
MSTSP24	60	36	9.857E-1	2	9.429E-1	1	8.068E-1	0
MSTSP25	66	26	9.089E-1	1	9.068E-1	1	7.469E-1	0
uni1+D5	11	2	9.576E-1	0	9.364E-1	0	1.000E+0	2
bays29+D5	39	2	1.000E+0	1	9.915E-1	1	3.812E-1	0
att48+D5	58	2	1.000E+0	2	9.859E-1	1	2.684E-1	0
gr24	24	2	1.000E+0	1	1.000E+0	1	8.292E-1	0
gr48	48	2	1.000E+0	2	9.757E-1	1	3.681E-1	0
Average Performance Score			1.03		0.63		0.53	

Figs. S.23-S.25 show the convergence plots (averaged over 30 runs) of the minimum objective value, RO, and DI obtained by TSPXEA-W, TSPXEA-ND, and NMA on MSTSP1, MSTSP8, MSTSP12, and MSTSP16. We can observe from these figures that NMA usually obtains a smaller minimum objective value than TSPXEA-ND and TSPXEA-W at the very early stage. However, TSPXEA-ND and TSPXEA-W converge more quickly at the later stage. NMA performs better than TSPXEA-ND and TSPXEA-W according to the results of RO and DI on MSTSP1. However, when the scale of the problem or the number of optimal solutions is larger (i.e., MSTSP8, MSTSP12, and MSTSP16), TSPXEA-ND and TSPXEA-W converge much more quickly than NMA according to the results of RO and DI.

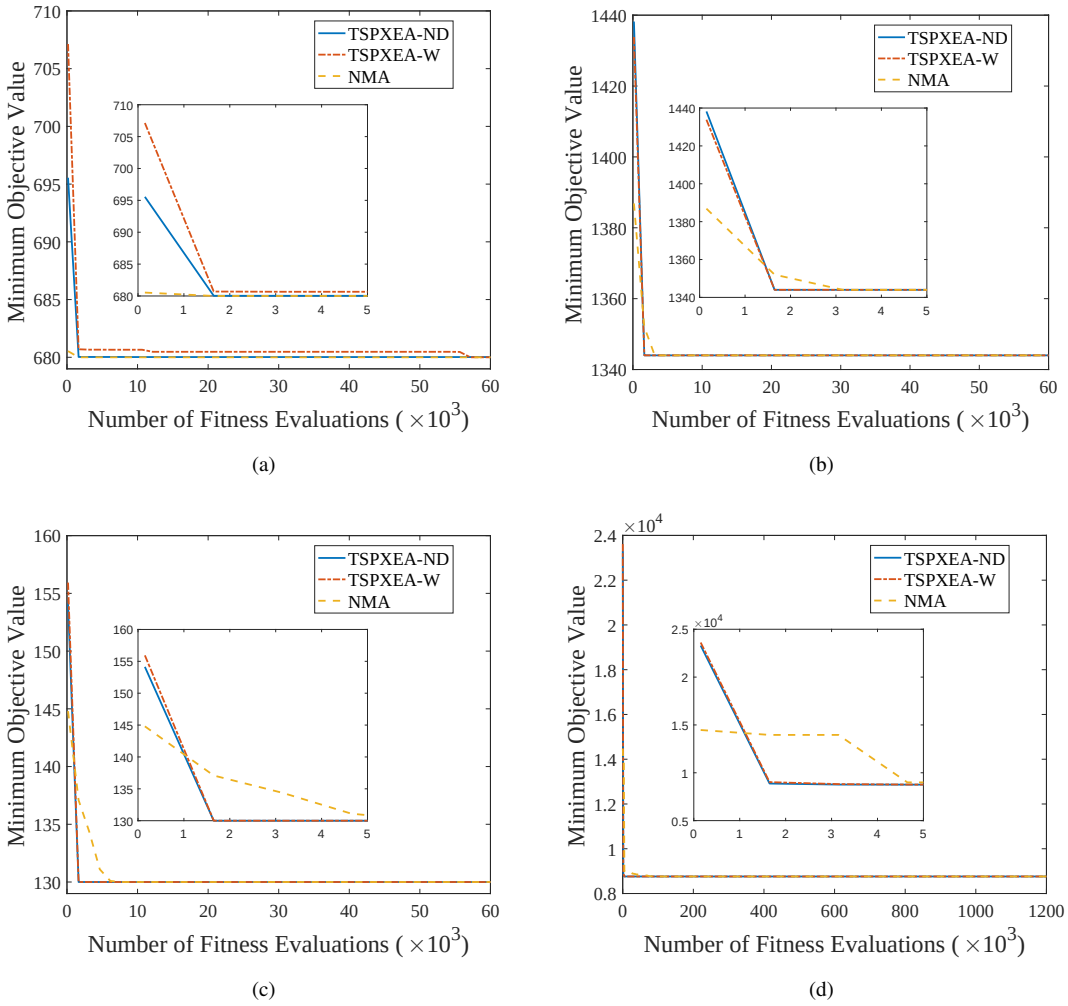

Fig. S.23. The convergence plots (averaged over 30 runs) of the minimum objective value obtained by TSPXEA-W, TSPXEA-ND, and NMA on MSTSP1. (a) MSTSPs. (b) MSTSP8. (c) MSTSP12. (d) MSTSP16.

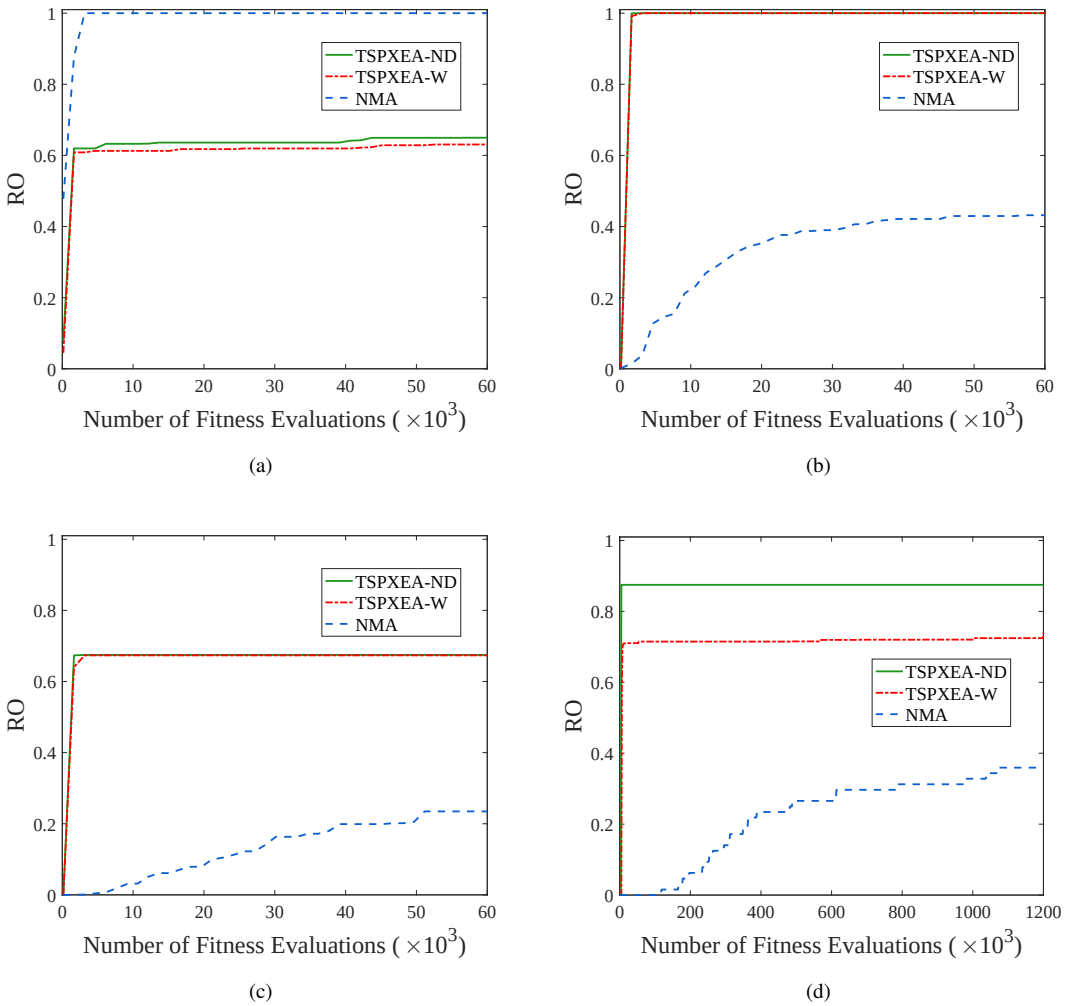

Fig. S.24. The convergence plots (averaged over 30 runs) of RO obtained by TSPXEA-W, TSPXEA-ND, and NMA on MSTSPs. (a) MSTSP1. (b) MSTSP8. (c) MSTSP12. (d) MSTSP16.

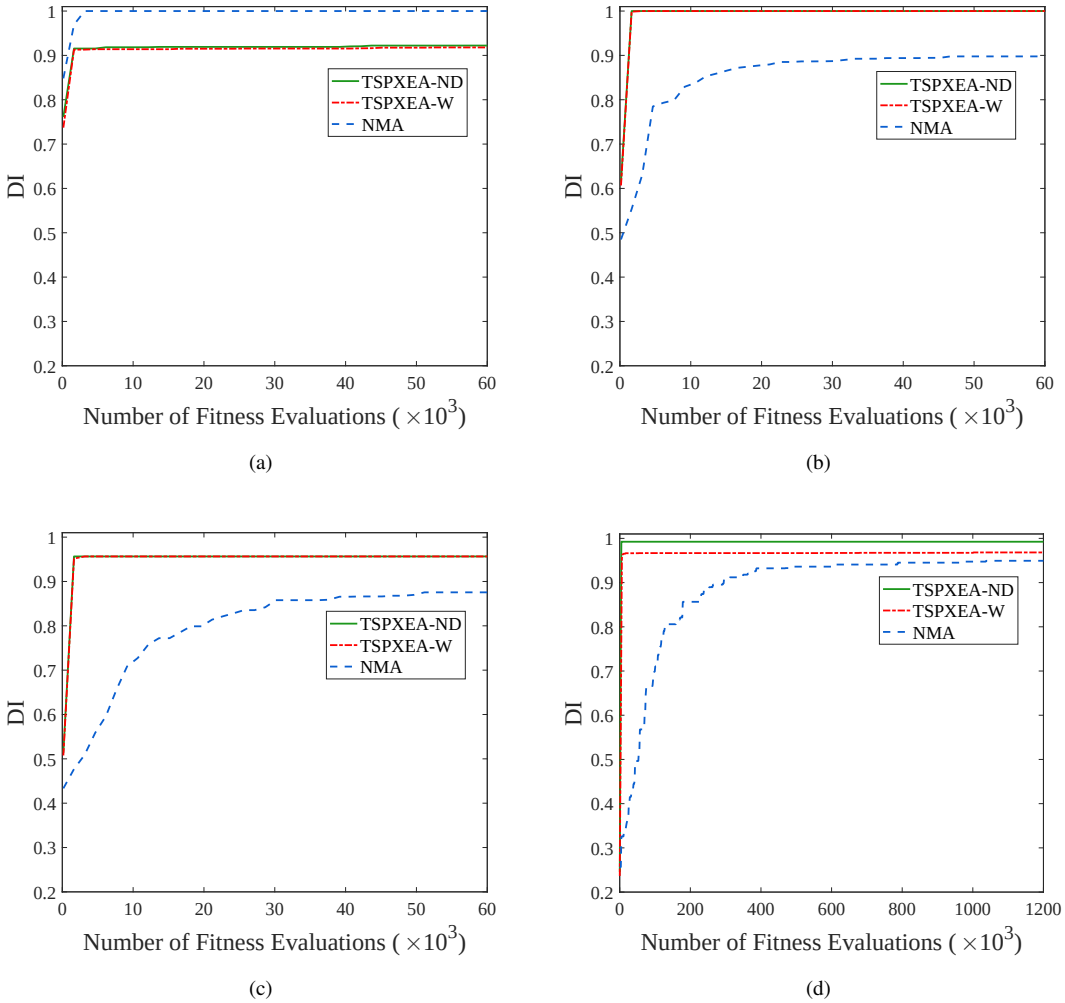

Fig. S.25. The convergence plots (averaged over 30 runs) of DI obtained by TSPXEA-W, TSPXEA-ND, and NMA on MSTSPs. (a) MSTSP1. (b) MSTSP8. (c) MSTSP12. (d) MSTSP16.

S-XII. Additional Figures and Tables

This section contains the following items:

- Fig. S.26 shows an illustration of EAX by Nagata and Obayashi [39].
- Figs. S.27-S.35 show the Pareto front (normalized to $[0, 1]$) of the test problems and the number of equivalent Pareto optimal solutions corresponding to each point on the Pareto front.
- Tables S.X-S.XII show the IGDM, HV, and GD results obtained by TSPXEA with different settings of η, respectively.
- Tables S.XIII and S.XIV show the mean values of HV and GD obtained by the comapred algorithms.

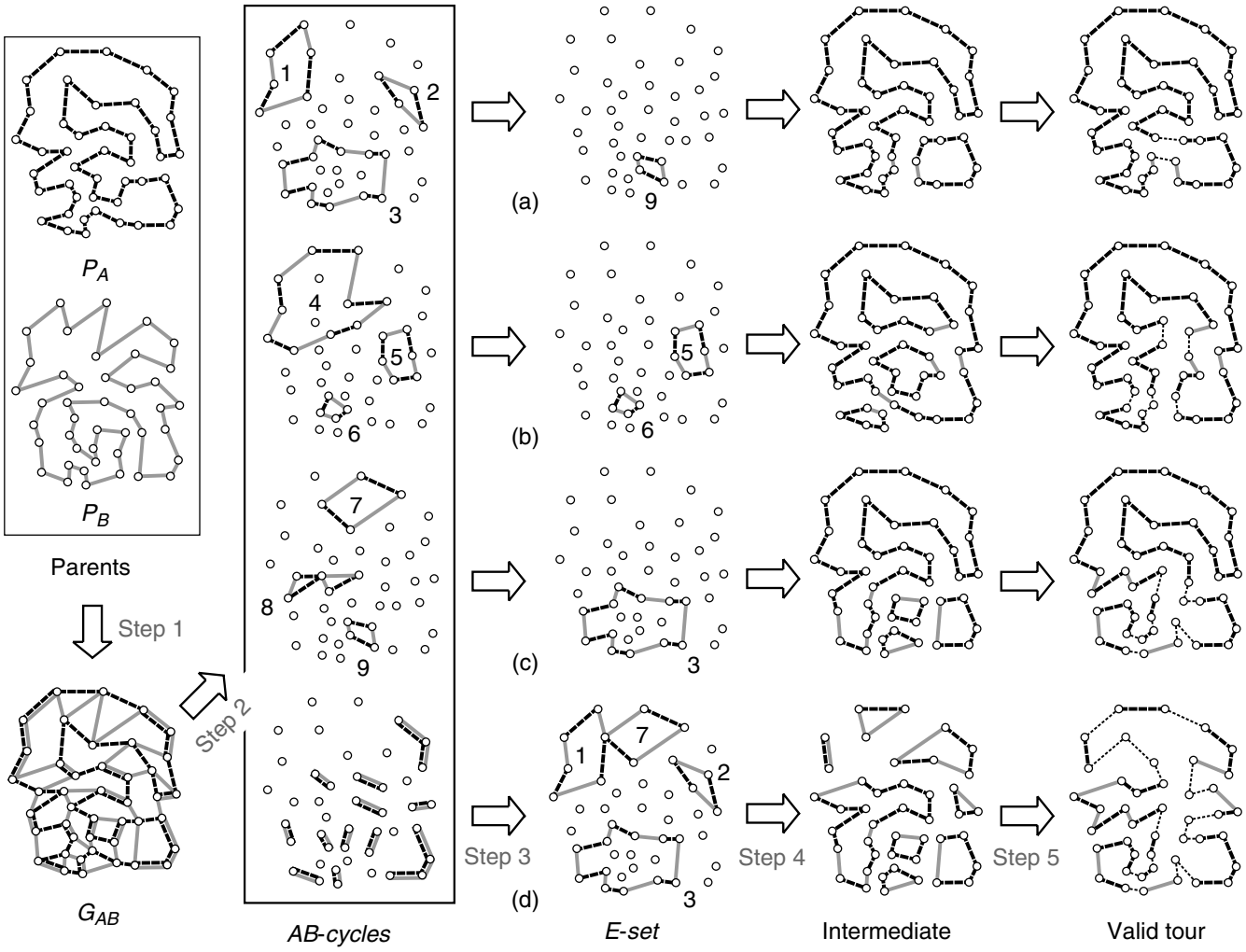

Fig. S.26. Illustration of EAX by Nagata and Obayashi [39].

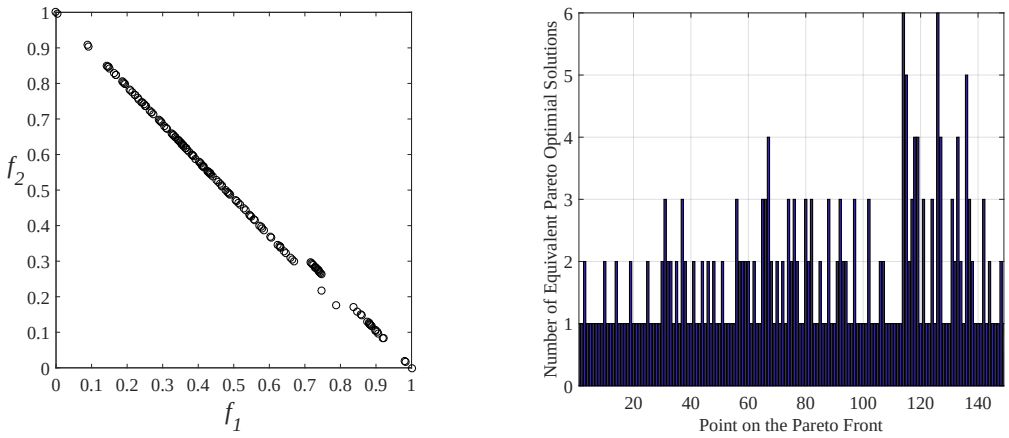

(a) (b)

Fig. S.27. (a) The Pareto front (normalized to $[0, 1]$) of an MMTSP whose D-type vertices are 'D2'. (b) The number of equivalent Pareto optimal solutions corresponding to each point on the Pareto front.

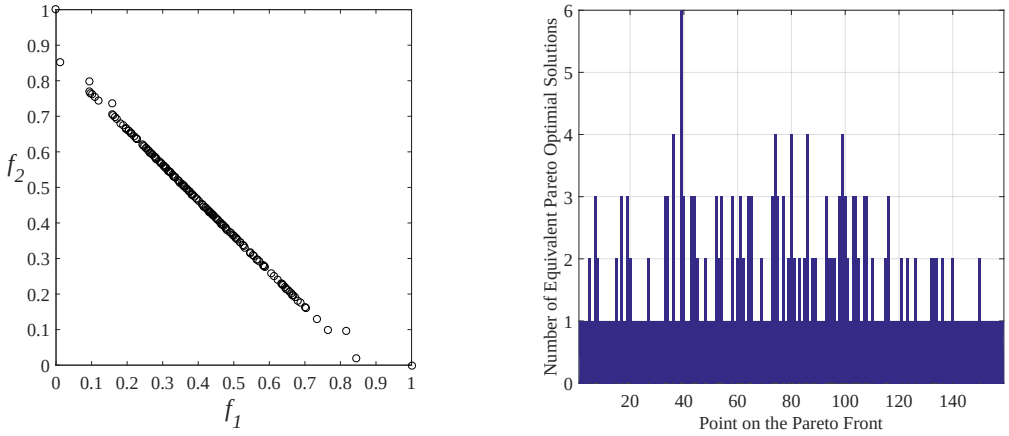

(a) (b)

Fig. S.28. (a) The Pareto front (normalized to $[0, 1]$) of an MMTSP whose D-type vertices are 'D3'. (b) The number of equivalent Pareto optimal solutions corresponding to each point on the Pareto front.

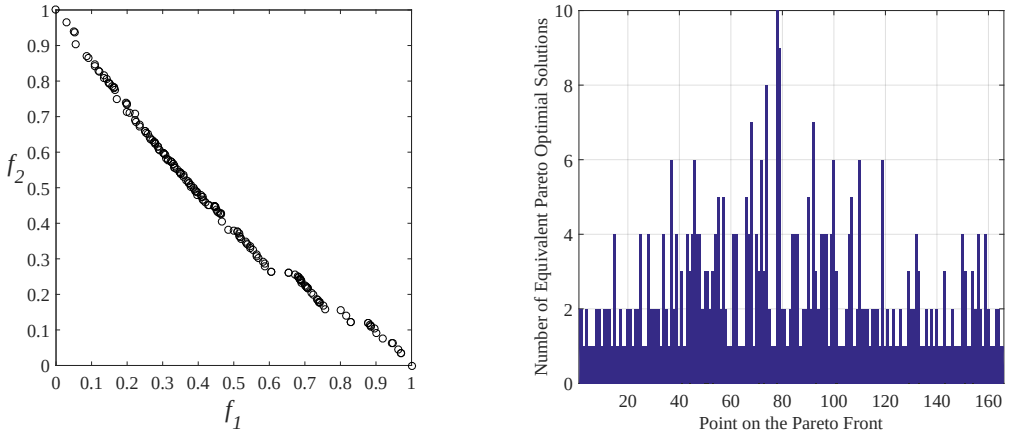

(a) (b)

Fig. S.29. (a) The Pareto front (normalized to $[0, 1]$) of an MMTSP whose D-type vertices are 'D4'. (b) The number of equivalent Pareto optimal solutions corresponding to each point on the Pareto front.

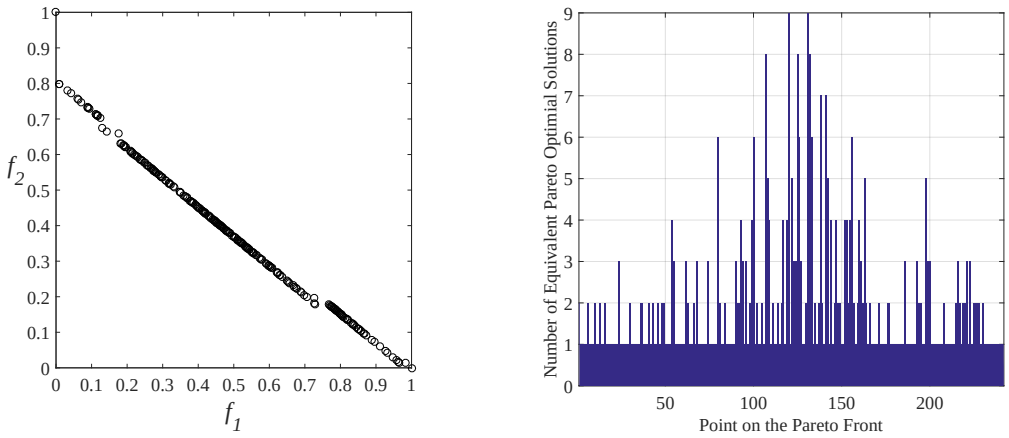

(a) (b)

Fig. S.30. (a) The Pareto front (normalized to $[0, 1]$) of an MMTSP whose D-type vertices are 'D5'. (b) The number of equivalent Pareto optimal solutions corresponding to each point on the Pareto front.

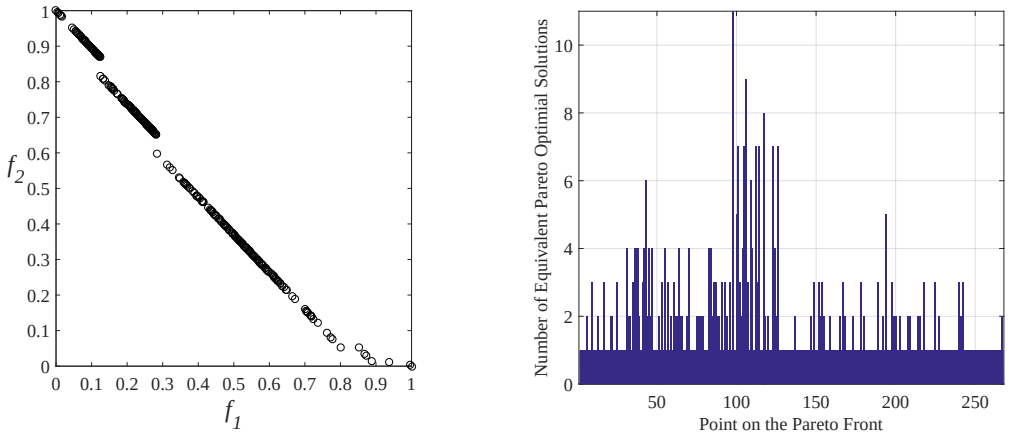

(a) (b)

Fig. S.31. (a) The Pareto front (normalized to $[0, 1]$) of an MMTSP whose D-type vertices are 'D6'. (b) The number of equivalent Pareto optimal solutions corresponding to each point on the Pareto front.

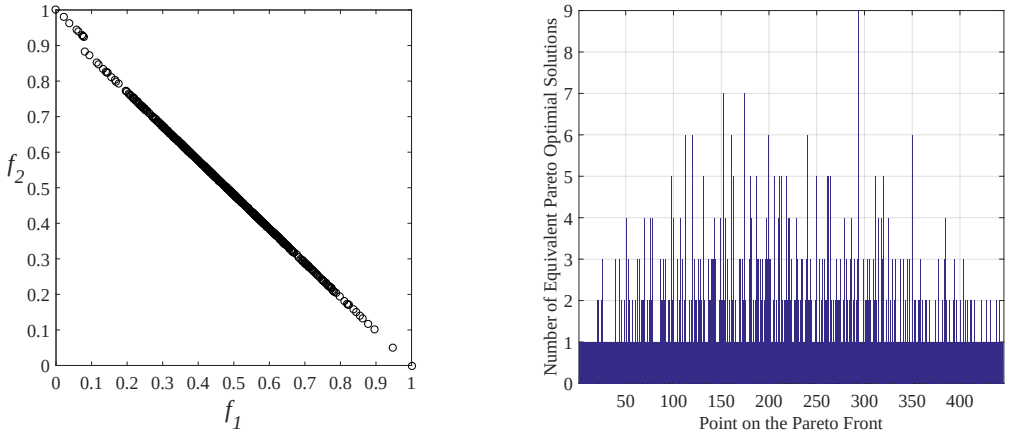

(a) (b)

Fig. S.32. (a) The Pareto front (normalized to $[0, 1]$) of an MMTSP whose D-type vertices are 'D7'. (b) The number of equivalent Pareto optimal solutions corresponding to each point on the Pareto front.

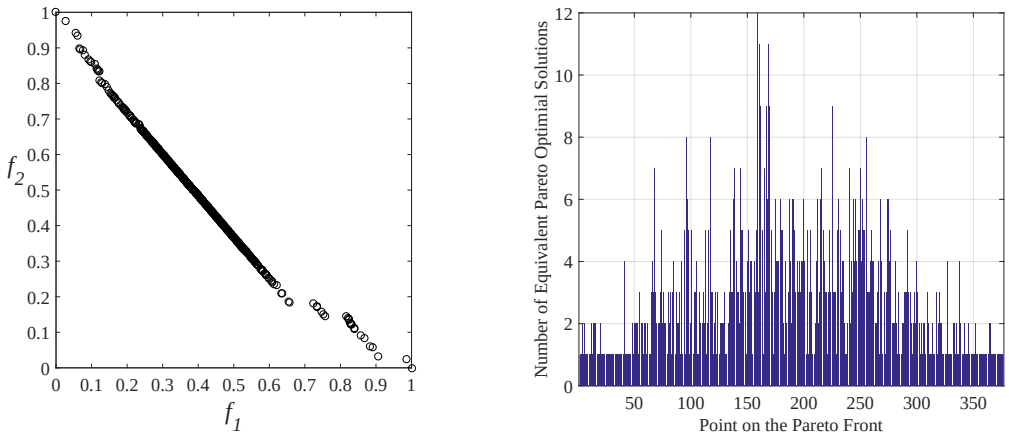

(a) (b)

Fig. S.33. (a) The Pareto front (normalized to $[0, 1]$) of an MMTSP whose D-type vertices are 'D8'. (b) The number of equivalent Pareto optimal solutions corresponding to each point on the Pareto front.

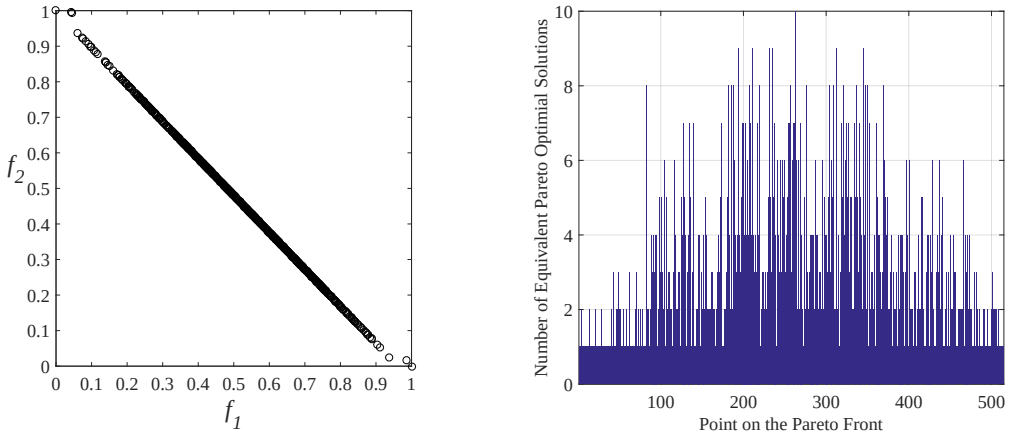

(a) (b)

Fig. S.34. (a) The Pareto front (normalized to $[0, 1]$) of an MMTSP whose D-type vertices are 'D9'. (b) The number of equivalent Pareto optimal solutions corresponding to each point on the Pareto front.

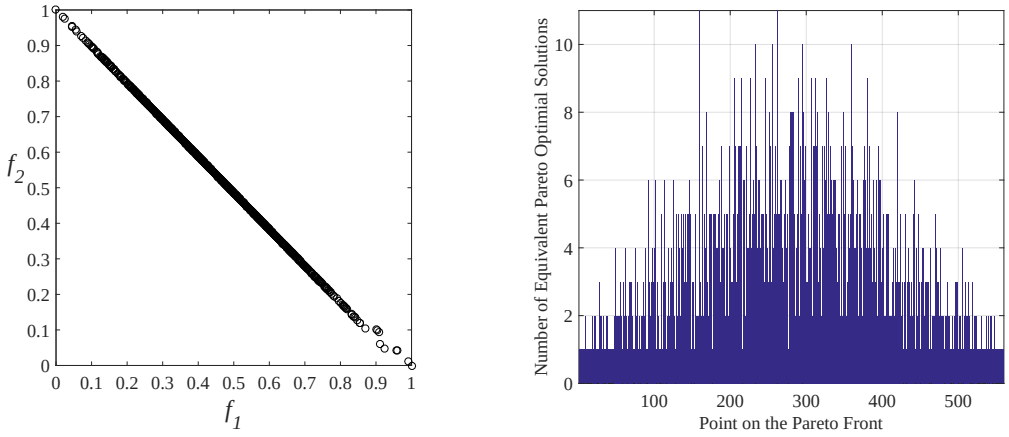

(a) (b)

Fig. S.35. (a) The Pareto front (normalized to $[0, 1]$) of an MMTSP whose D-type vertices are 'D10'. (b) The number of equivalent Pareto optimal solutions corresponding to each point on the Pareto front.

TABLE S.X
THE MEAN IGDM VALUES AND THE PERFORMANCE SCORES OBTAINED BY TSPXEA WITH DIFFERENT SETTINGS OF η.

IGDM	η=0		η=0.1		η=0.2		η=0.3		η=0.4		η=0.5		η=0.6		η=0.7		η=0.8		η=0.9		η=1	
uni1+D1	7.819E-3	1	8.075E-3	0	7.757E-3	3	7.761E-3	2	8.186E-3	0	8.047E-3	0	8.317E-3	0	8.282E-3	0	7.980E-3	0	7.885E-3	0	8.276E-3	0
uni1+D2	1.676E-2	0	1.597E-2	0	1.530E-2	0	1.528E-2	0	1.647E-2	0	1.637E-2	0	1.511E-2	0	1.588E-2	0	1.604E-2	0	1.596E-2	0	1.550E-2	0
uni1+D3	4.069E-3	1	4.236E-3	1	4.190E-3	1	4.234E-3	1	4.169E-3	1	4.302E-3	1	4.266E-3	1	4.256E-3	1	4.146E-3	1	4.111E-3	1	6.223E-3	0
uni1+D4	9.826E-3	3	9.932E-3	2	1.001E-2	1	1.022E-2	1	1.013E-2	1	1.057E-2	1	1.030E-2	1	1.026E-2	1	1.031E-2	1	1.003E-2	1	1.608E-2	0
uni1+D5	8.788E-3	10	1.021E-2	1	1.030E-2	1	9.851E-3	2	9.943E-3	1	1.050E-2	1	9.765E-3	2	1.003E-2	1	9.639E-3	2	1.002E-2	1	1.440E-2	0
uni1+D6	9.494E-3	1	8.947E-3	2	9.149E-3	2	9.088E-3	2	8.981E-3	2	8.827E-3	2	8.364E-3	3	8.883E-3	2	9.279E-3	1	1.009E-2	1	2.730E-2	0
uni1+D7	7.311E-3	0	7.322E-3	0	6.728E-3	7	7.428E-3	0	7.132E-3	0	7.211E-3	0	7.396E-3	0	6.882E-3	2	7.071E-3	0	7.167E-3	0	7.778E-3	0
uni1+D8	8.284E-3	1	8.326E-3	1	8.381E-3	1	8.304E-3	1	8.292E-3	1	8.112E-3	1	8.187E-3	1	8.106E-3	1	8.194E-3	1	8.352E-3	1	2.441E-2	0
uni1+D9	9.066E-3	0	9.149E-3	0	9.468E-3	0	9.083E-3	0	9.001E-3	0	8.879E-3	1	9.094E-3	0	9.163E-3	0	8.751E-3	1	8.874E-3	1	9.226E-3	0
uni1+D10	8.993E-3	0	9.198E-3	0	9.005E-3	0	9.041E-3	0	8.614E-3	4	9.064E-3	0	9.041E-3	0	9.184E-3	0	9.178E-3	0	8.584E-3	6	9.170E-3	0
APS (uni1)	1.7		0.7		1.6		0.9		1.0		0.7		0.8		0.8		0.7		1.2		0.0	
att48+D1	8.160E-3	5	9.738E-3	1	9.927E-3	1	9.538E-3	1	9.746E-3	1	9.247E-3	1	8.361E-3	3	9.229E-3	1	9.118E-3	1	8.977E-3	1	2.410E-2	0
att48+D2	1.726E-2	0	1.634E-2	0	1.783E-2	0	1.725E-2	0	1.651E-2	0	1.559E-2	0	1.803E-2	0	1.714E-2	0	1.689E-2	0	1.688E-2	0	1.869E-2	0
att48+D3	5.609E-3	3	7.452E-3	1	5.680E-3	3	6.423E-3	1	6.021E-3	1	5.934E-3	1	7.385E-3	1	6.654E-3	1	6.613E-3	1	5.639E-3	1	1.292E-2	0
att48+D4	8.197E-3	3	8.352E-3	1	8.880E-3	1	8.562E-3	1	8.675E-3	1	8.380E-3	1	8.640E-3	1	9.198E-3	1	8.508E-3	1	9.176E-3	1	1.583E-2	0
att48+D5	1.045E-2	1	9.998E-3	1	1.158E-2	1	9.813E-3	1	1.034E-2	1	1.061E-2	1	1.023E-2	1	1.017E-2	1	1.034E-2	1	1.033E-2	1	1.670E-2	0
att48+D6	1.158E-2	1	1.287E-2	1	1.009E-2	4	1.117E-2	4	1.169E-2	1	1.218E-2	1	1.093E-2	1	1.134E-2	1	1.203E-2	1	1.356E-2	1	3.195E-2	0
att48+D7	6.976E-3	1	6.559E-3	4	7.964E-3	1	7.439E-3	1	7.063E-3	1	7.625E-3	1	7.488E-3	1	7.011E-3	1	7.896E-3	1	7.210E-3	1	9.321E-3	0
att48+D8	1.087E-2	1	9.262E-3	1	1.120E-2	1	9.356E-3	3	1.075E-2	1	1.147E-2	1	1.027E-2	1	1.167E-2	1	1.035E-2	1	1.249E-2	1	4.435E-2	0
att48+D9	9.745E-3	0	1.065E-2	0	9.989E-3	0	1.045E-2	0	9.230E-3	3	1.024E-2	0	1.032E-2	0	1.057E-2	0	9.816E-3	1	1.175E-2	0	1.138E-2	0
att48+D10	9.989E-3	1	9.911E-3	1	1.012E-2	1	1.013E-2	1	9.947E-3	3	1.008E-2	1	9.927E-3	1	9.879E-3	1	9.515E-3	1	9.311E-3	2	1.339E-2	0
APS(att48)	1.6		1.1		1.3		1.3		1.3		0.8		1.0		0.8		0.9		0.9		0.0	
lin105+D1	1.874E-2	9	2.603E-2	5	3.503E-2	1	4.538E-2	0	3.643E-2	0	3.504E-2	1	3.404E-2	1	2.984E-2	1	3.688E-2	0	3.883E-2	0	3.893E-2	0
lin105+D2	4.265E-2	7	4.755E-2	6	6.164E-2	0	7.145E-2	0	6.495E-2	0	6.860E-2	0	6.778E-2	0	7.427E-2	0	7.609E-2	0	6.808E-2	0	6.372E-2	0
lin105+D3	2.231E-2	9	3.798E-2	4	5.837E-2	0	6.046E-2	0	5.315E-2	0	4.811E-2	1	4.034E-2	3	7.198E-2	0	3.924E-2	6	6.606E-2	0	5.855E-2	0
lin105+D4	1.181E-2	9	1.401E-2	9	2.357E-2	0	2.662E-2	0	2.490E-2	0	2.525E-2	0	2.290E-2	1	2.725E-2	0	2.487E-2	0	2.802E-2	0	2.672E-2	0
lin105+D5	1.864E-2	10	2.927E-2	7	5.932E-2	0	5.334E-2	0	5.514E-2	0	5.051E-2	0	6.038E-2	0	5.016E-2	0	4.616E-2	0	5.193E-2	0	5.500E-2	0
lin105+D6	2.747E-2	8	2.942E-2	8	5.232E-2	0	3.687E-2	5	6.750E-2	0	5.274E-2	0	5.411E-2	0	5.414E-2	0	6.135E-2	0	6.736E-2	0	5.763E-2	0
lin105+D7	1.197E-2	8	1.404E-2	6	1.697E-2	0	1.590E-2	0	1.891E-2	0	2.074E-2	0	1.948E-2	0	1.821E-2	0	1.578E-2	1	1.777E-2	0	2.133E-2	0
lin105+D8	2.075E-2	9	2.029E-2	8	3.612E-2	1	4.038E-2	1	4.028E-2	1	4.020E-2	1	4.416E-2	1	3.909E-2	1	4.563E-2	1	4.014E-2	1	7.276E-2	0
lin105+D9	2.603E-2	8	2.127E-2	9	5.705E-2	0	6.124E-2	0	4.605E-2	0	5.180E-2	0	5.368E-2	0	3.978E-2	0	4.277E-2	0	5.591E-2	0	4.407E-2	0
lin105+D10	1.705E-2	7	2.043E-2	4	2.951E-2	0	3.611E-2	0	2.975E-2	0	2.472E-2	0	3.162E-2	0	2.659E-2	0	2.781E-2	0	3.019E-2	0	2.812E-2	0
APS(lin105)	8.4		6.6		0.2		0.6		0.1		0.3		0.6		0.2		0.8		0.1		0.0	
a280+D1	3.652E-2	0	3.451E-2	3	3.318E-2	5	3.669E-2	0	3.694E-2	0	3.706E-2	0	3.751E-2	0	3.801E-2	0	4.014E-2	0	3.630E-2	0	3.112E-2	10
a280+D2	2.475E-2	8	2.625E-2	7	2.915E-2	5	3.451E-2	0	3.831E-2	0	3.599E-2	0	3.989E-2	0	3.790E-2	0	3.890E-2	0	3.707E-2	0	3.368E-2	0
a280+D3	2.242E-2	8	2.118E-2	8	2.294E-2	8	3.802E-2	1	3.662E-2	2	4.405E-2	0	4.631E-2	0	4.193E-2	0	3.909E-2	1	3.279E-2	4	5.738E-2	0
a280+D4	2.492E-2	8	2.635E-2	3	2.586E-2	4	2.854E-2	0	2.944E-2	0	2.942E-2	0	2.852E-2	0	2.916E-2	0	2.793E-2	0	2.809E-2	0	2.559E-2	6
a280+D5	2.059E-2	9	2.181E-2	8	2.432E-2	8	3.229E-2	0	3.330E-2	0	3.766E-2	0	2.889E-2	2	3.369E-2	0	3.546E-2	0	3.302E-2	0	3.388E-2	0
a280+D6	2.824E-2	8	2.807E-2	8	3.034E-2	8	4.407E-2	0	4.024E-2	1	4.673E-2	0	4.746E-2	0	3.906E-2	1	4.519E-2	0	4.171E-2	1	5.546E-2	0
a280+D7	1.495E-2	8	1.557E-2	5	1.628E-2	0	1.721E-2	0	1.705E-2	0	1.790E-2	0	1.657E-2	0	1.664E-2	0	1.697E-2	0	1.825E-2	0	1.660E-2	2
a280+D8	2.005E-2	8	2.031E-2	8	2.209E-2	8	2.842E-2	2	3.134E-2	1	3.008E-2	1	3.167E-2	1	2.811E-2	2	2.885E-2	2	3.513E-2	1	5.335E-2	0
a280+D9	1.822E-2	8	1.849E-2	8	1.981E-2	8	2.452E-2	0	2.516E-2	0	2.360E-2	0	2.573E-2	0	2.565E-2	0	2.735E-2	0	2.674E-2	0	3.617E-2	0
a280+D10	1.456E-2	8	1.588E-2	8	1.518E-2	8	1.994E-2	0	2.264E-2	0	2.113E-2	0	1.999E-2	0	2.071E-2	0	2.105E-2	0	2.003E-2	0	2.111E-2	0
APS(a280)	7.3		6.6		6.2		0.3		0.4		0.1		0.3		0.3		0.3		0.6		1.8	
APS(all)	4.8		3.8		2.3		0.8		0.7		0.5		0.7		0.5		0.7		0.7		0.5	

APS is short for Average Performance Score.

TABLE S.XI
THE MEAN HV VALUES AND THE PERFORMANCE SCORES OBTAINED BY TSPXEA WITH DIFFERENT SETTINGS OF η.

HV	η=0		η=0.1		η=0.2		η=0.3		η=0.4		η=0.5		η=0.6		η=0.7		η=0.8		η=0.9		η=1	
uni1+D1	9.954E-1	0	9.953E-1	0	9.951E-1	0	9.954E-1	0	9.953E-1	0	9.951E-1	0	9.954E-1	0	9.952E-1	0	9.952E-1	0	9.950E-1	0	9.950E-1	0
uni1+D2	9.846E-1	0	9.828E-1	0	9.842E-1	0	9.847E-1	0	9.834E-1	0	9.828E-1	0	9.843E-1	0	9.840E-1	0	9.840E-1	0	9.839E-1	0	9.848E-1	0
uni1+D3	9.981E-1	1	9.984E-1	2	9.984E-1	2	9.985E-1	2	9.985E-1	2	9.984E-1	2	9.983E-1	1	9.981E-1	1	9.985E-1	2	9.986E-1	2	9.970E-1	0
uni1+D4	9.944E-1	8	9.937E-1	3	9.939E-1	6	9.931E-1	1	9.934E-1	1	9.928E-1	1	9.931E-1	1	9.929E-1	1	9.931E-1	1	9.934E-1	1	9.849E-1	0
uni1+D5	9.943E-1	1	9.933E-1	1	9.935E-1	1	9.940E-1	1	9.934E-1	1	9.929E-1	1	9.930E-1	1	9.935E-1	1	9.930E-1	1	9.936E-1	1	9.904E-1	0
uni1+D6	9.925E-1	1	9.931E-1	2	9.931E-1	2	9.932E-1	2	9.934E-1	3	9.931E-1	2	9.939E-1	7	9.930E-1	1	9.930E-1	2	9.918E-1	1	9.744E-1	0
uni1+D7	9.899E-1	0	9.906E-1	0	9.922E-1	5	9.901E-1	0	9.912E-1	2	9.917E-1	3	9.902E-1	0	9.911E-1	1	9.921E-1	5	9.915E-1	2	9.894E-1	0
uni1+D8	9.930E-1	3	9.931E-1	3	9.928E-1	2	9.928E-1	2	9.929E-1	3	9.926E-1	2	9.928E-1	2	9.927E-1	2	9.922E-1	1	9.916E-1	1	9.690E-1	0
uni1+D9	9.934E-1	0	9.935E-1	1	9.935E-1	0	9.937E-1	2	9.938E-1	3	9.934E-1	0	9.937E-1	2	9.935E-1	1	9.936E-1	1	9.936E-1	1	9.931E-1	0
uni1+D10	9.933E-1	1	9.935E-1	1	9.934E-1	1	9.934E-1	0	9.936E-1	3	9.936E-1	1	9.936E-1	2	9.935E-1	1	9.933E-1	0	9.936E-1	1	9.916E-1	0
APS (uni1)	1.5		1.3		1.9		1.0		1.8		1.2		1.6		0.9		1.3		1.0		0.0	
att48+D1	9.943E-1	2	9.901E-1	1	9.902E-1	1	9.907E-1	1	9.907E-1	1	9.913E-1	1	9.935E-1	1	9.920E-1	1	9.918E-1	1	9.927E-1	1	9.647E-1	0
att48+D2	9.826E-1	1	9.812E-1	1	9.768E-1	0	9.774E-1	0	9.805E-1	1	9.825E-1	2	9.766E-1	0	9.791E-1	0	9.781E-1	0	9.787E-1	1	9.727E-1	0
att48+D3	9.948E-1	4	9.918E-1	1	9.952E-1	1	9.938E-1	1	9.942E-1	1	9.945E-1	1	9.914E-1	1	9.939E-1	1	9.930E-1	1	9.953E-1	2	9.767E-1	0
att48+D4	9.949E-1	2	9.930E-1	1	9.919E-1	1	9.933E-1	1	9.930E-1	1	9.938E-1	1	9.924E-1	1	9.924E-1	1	9.941E-1	2	9.928E-1	1	9.845E-1	0
att48+D5	9.871E-1	0	9.900E-1	0	9.847E-1	0	9.887E-1	0	9.885E-1	0	9.870E-1	0	9.883E-1	0	9.886E-1	0	9.881E-1	0	9.882E-1	0	9.866E-1	0
att48+D6	9.871E-1	1	9.834E-1	1	9.908E-1	4	9.872E-1	1	9.860E-1	1	9.854E-1	1	9.902E-1	3	9.892E-1	2	9.883E-1	1	9.854E-1	1	9.639E-1	0
att48+D7	9.949E-1	1	9.953E-1	1	9.918E-1	1	9.935E-1	1	9.944E-1	1	9.931E-1	1	9.939E-1	1	9.938E-1	1	9.925E-1	1	9.934E-1	1	9.837E-1	0
att48+D8	9.869E-1	1	9.915E-1	1	9.864E-1	1	9.919E-1	2	9.883E-1	1	9.864E-1	1	9.889E-1	1	9.855E-1	1	9.885E-1	1	9.838E-1	1	9.368E-1	0
att48+D9	9.905E-1	0	9.889E-1	0	9.896E-1	0	9.889E-1	0	9.913E-1	1	9.905E-1	0	9.893E-1	0	9.887E-1	0	9.896E-1	0	9.856E-1	0	9.857E-1	0
att48+D10	9.912E-1	1	9.916E-1	1	9.902E-1	1	9.908E-1	1	9.908E-1	1	9.914E-1	1	9.906E-1	1	9.911E-1	1	9.924E-1	1	9.919E-1	1	9.831E-1	0
APS(att48)	1.3		0.8		1.0		0.8		0.9		0.9		0.9		0.8		0.8		0.9		0.0	
lin105+D1	9.704E-1	9	9.549E-1	3	9.366E-1	1	9.154E-1	0	9.333E-1	0	9.370E-1	1	9.381E-1	1	9.468E-1	1	9.327E-1	1	9.293E-1	0	9.295E-1	0
lin105+D2	9.157E-1	8	9.007E-1	4	8.685E-1	0	8.487E-1	0	8.631E-1	0	8.534E-1	0	8.569E-1	0	8.448E-1	0	8.360E-1	0	8.557E-1	0	8.659E-1	0
lin105+D3	9.613E-1	9	9.305E-1	4	8.925E-1	0	8.888E-1	0	9.026E-1	0	9.120E-1	1	9.268E-1	4	8.672E-1	0	9.296E-1	5	8.788E-1	0	8.898E-1	0
lin105+D4	9.851E-1	9	9.793E-1	9	9.577E-1	0	9.503E-1	0	9.550E-1	0	9.541E-1	0	9.596E-1	0	9.501E-1	0	9.555E-1	0	9.475E-1	0	9.550E-1	0
lin105+D5	9.701E-1	10	9.463E-1	7	8.868E-1	0	8.980E-1	0	8.966E-1	0	9.042E-1	0	8.856E-1	0	9.050E-1	0	9.130E-1	0	9.014E-1	0	8.985E-1	0
lin105+D6	9.520E-1	8	9.482E-1	8	8.981E-1	0	9.312E-1	4	8.693E-1	0	8.992E-1	0	8.967E-1	0	8.957E-1	0	8.841E-1	0	8.689E-1	0	9.027E-1	0
lin105+D7	9.807E-1	8	9.768E-1	8	9.688E-1	0	9.700E-1	0	9.643E-1	0	9.599E-1	0	9.624E-1	0	9.665E-1	0	9.722E-1	2	9.664E-1	0	9.575E-1	0
lin105+D8	9.634E-1	9	9.644E-1	9	9.292E-1	1	9.200E-1	1	9.202E-1	1	9.213E-1	1	9.126E-1	1	9.231E-1	1	9.082E-1	1	9.213E-1	1	8.652E-1	0
lin105+D9	9.511E-1	9	9.612E-1	9	8.791E-1	0	8.715E-1	0	9.034E-1	0	8.893E-1	0	8.883E-1	0	9.181E-1	0	9.112E-1	0	8.815E-1	0	9.076E-1	0
lin105+D10	9.700E-1	7	9.611E-1	5	9.378E-1	0	9.236E-1	0	9.382E-1	0	9.508E-1	1	9.335E-1	0	9.462E-1	0	9.434E-1	0	9.363E-1	0	9.411E-1	0
APS(lin105)	8.6		6.6		0.2		0.5		0.1		0.4		0.6		0.2		0.9		0.1		0.0	
a280+D1	9.666E-1	7	9.673E-1	7	9.704E-1	7	9.577E-1	0	9.586E-1	0	9.566E-1	0	9.547E-1	0	9.550E-1	0	9.541E-1	0	9.588E-1	0	9.668E-1	7
a280+D2	9.713E-1	8	9.693E-1	8	9.630E-1	8	9.402E-1	0	9.332E-1	0	9.355E-1	0	9.261E-1	0	9.315E-1	0	9.270E-1	0	9.330E-1	0	9.352E-1	0
a280+D3	9.590E-1	8	9.690E-1	10	9.569E-1	8	9.208E-1	0	9.291E-1	1	9.105E-1	0	9.083E-1	0	9.136E-1	0	9.238E-1	0	9.359E-1	4	8.987E-1	0
a280+D4	9.772E-1	8	9.775E-1	8	9.748E-1	7	9.677E-1	0	9.697E-1	0	9.646E-1	0	9.670E-1	0	9.667E-1	0	9.670E-1	0	9.648E-1	0	9.729E-1	5
a280+D5	9.751E-1	9	9.726E-1	9	9.616E-1	8	9.438E-1	1	9.375E-1	0	9.288E-1	0	9.476E-1	2	9.365E-1	0	9.335E-1	0	9.433E-1	1	9.494E-1	2
a280+D6	9.599E-1	9	9.591E-1	9	9.494E-1	8	9.147E-1	0	9.262E-1	0	9.097E-1	0	9.075E-1	0	9.279E-1	0	9.119E-1	0	9.217E-1	0	9.031E-1	0
a280+D7	9.801E-1	9	9.794E-1	9	9.765E-1	3	9.715E-1	0	9.721E-1	0	9.707E-1	0	9.737E-1	0	9.726E-1	0	9.725E-1	0	9.691E-1	0	9.701E-1	0
a280+D8	9.727E-1	9	9.718E-1	8	9.663E-1	8	9.474E-1	1	9.414E-1	1	9.437E-1	1	9.389E-1	1	9.488E-1	2	9.476E-1	2	9.317E-1	1	9.126E-1	0
a280+D9	9.763E-1	9	9.749E-1	8	9.709E-1	8	9.564E-1	0	9.544E-1	0	9.571E-1	0	9.525E-1	0	9.526E-1	0	9.480E-1	0	9.472E-1	0	9.400E-1	0
a280+D10	9.787E-1	8	9.754E-1	8	9.777E-1	8	9.633E-1	0	9.552E-1	0	9.594E-1	0	9.620E-1	0	9.605E-1	0	9.587E-1	0	9.627E-1	0	9.570E-1	0
APS(a280)	8.4		8.4		7.3		0.2		0.2		0.1		0.3		0.2		0.2		0.6		1.4	
APS(all)	5.0		4.3		2.6		0.6		0.8		0.7		0.9		0.5		0.8		0.7		0.4	

APS is short for Average Performance Score.

TABLE S.XII
THE MEAN GD VALUES AND THE PERFORMANCE SCORES OBTAINED BY TSPXEA WITH DIFFERENT SETTINGS OF η.

GD	η=0		η=0.1		η=0.2		η=0.3		η=0.4		η=0.5		η=0.6		η=0.7		η=0.8		η=0.9		η=1	
uni1+D1	3.644E-4	0	3.646E-4	0	3.809E-4	0	3.709E-4	0	3.680E-4	0	3.715E-4	0	3.813E-4	0	3.785E-4	0	3.949E-4	0	4.016E-4	0	3.531E-4	1
uni1+D2	1.505E-3	0	1.571E-3	0	1.492E-3	0	1.538E-3	0	1.568E-3	0	1.637E-3	0	1.522E-3	0	1.601E-3	0	1.592E-3	0	1.512E-3	0	1.046E-3	10
uni1+D3	2.363E-4	0	9.619E-5	1	9.751E-5	1	8.093E-5	1	6.762E-5	1	9.684E-5	1	1.293E-4	0	1.765E-4	0	6.565E-5	1	4.974E-5	2	1.121E-4	1
uni1+D4	4.788E-4	9	6.005E-4	1	6.127E-4	0	6.366E-4	0	6.476E-4	0	6.396E-4	0	6.371E-4	0	6.696E-4	0	6.704E-4	0	6.698E-4	0	4.060E-4	9
uni1+D5	1.038E-4	0	1.219E-4	0	1.856E-4	0	1.016E-4	0	1.935E-4	0	1.739E-4	0	1.940E-4	0	1.686E-4	0	1.734E-4	0	1.372E-4	0	3.786E-5	5
uni1+D6	3.443E-4	1	1.363E-4	3	2.025E-4	1	2.383E-4	1	2.313E-4	1	1.934E-4	1	1.298E-4	2	2.614E-4	1	1.609E-4	1	3.299E-4	1	8.676E-4	0
uni1+D7	5.984E-4	0	5.242E-4	0	1.429E-4	8	6.820E-4	0	5.848E-4	0	4.585E-4	0	7.194E-4	0	5.463E-4	0	3.152E-4	2	3.952E-4	0	4.450E-4	0
uni1+D8	2.806E-4	0	2.415E-4	0	2.452E-4	0	2.380E-4	0	2.475E-4	0	2.383E-4	0	2.245E-4	1	2.454E-4	0	2.418E-4	0	2.690E-4	0	1.589E-4	10
uni1+D9	0.000E+0	0	1.628E-5	0	9.156E-6	0	0.000E+0	0	1.829E-5	0	0.000E+0	0	0.000E+0	0	0.000E+0	0	9.156E-6	0	9.144E-6	0	0.000E+0	0
uni1+D10	8.547E-5	0	6.758E-6	0	2.594E-5	0	2.308E-5	0	1.349E-5	0	1.348E-5	0	1.167E-5	0	9.607E-6	0	1.916E-5	0	1.348E-5	0	2.250E-4	0
APS (uni1)	1.0		0.5		1.0		0.2		0.2		0.2		0.3		0.1		0.4		0.3		3.6	
att48+D1	3.671E-4	7	5.793E-4	1	5.705E-4	1	5.187E-4	1	5.455E-4	1	4.900E-4	1	3.936E-4	6	4.612E-4	1	5.298E-4	1	4.695E-4	1	7.232E-4	0
att48+D2	1.079E-3	3	1.106E-3	3	1.609E-3	0	1.558E-3	0	1.288E-3	0	1.116E-3	3	1.567E-3	0	1.318E-3	0	1.441E-3	0	1.427E-3	0	6.814E-4	10
att48+D3	2.138E-4	0	3.685E-4	0	1.894E-4	0	2.649E-4	0	2.352E-4	0	2.241E-4	0	3.876E-4	0	2.576E-4	0	3.025E-4	0	1.834E-4	0	1.885E-4	0
att48+D4	2.357E-4	0	2.908E-4	0	3.513E-4	0	2.562E-4	0	3.025E-4	0	2.770E-4	0	3.257E-4	0	2.946E-4	0	2.457E-4	0	2.813E-4	0	2.186E-4	3
att48+D5	5.051E-4	0	3.286E-4	0	6.101E-4	0	4.163E-4	0	3.964E-4	0	4.692E-4	0	3.974E-4	0	4.454E-4	0	4.150E-4	0	3.611E-4	0	2.787E-4	8
att48+D6	4.237E-4	0	6.180E-4	0	2.402E-4	2	4.194E-4	0	4.786E-4	0	4.761E-4	0	2.839E-4	1	3.595E-4	0	3.914E-4	0	6.117E-4	0	5.974E-4	0
att48+D7	3.358E-5	1	1.848E-5	1	1.833E-4	1	9.983E-5	1	6.207E-5	1	1.273E-4	1	8.112E-5	1	8.970E-5	1	1.448E-4	1	6.584E-5	1	3.857E-4	0
att48+D8	5.577E-4	0	3.607E-4	1	5.914E-4	0	3.645E-4	1	5.113E-4	0	5.895E-4	0	4.931E-4	1	6.251E-4	0	5.050E-4	1	7.075E-4	0	5.110E-4	6
att48+D9	1.544E-4	0	2.103E-4	0	1.991E-4	0	2.211E-4	0	1.141E-4	0	1.539E-4	0	2.053E-4	0	2.457E-4	0	1.740E-4	0	3.744E-4	0	3.218E-4	0
att48+D10	8.640E-5	0	6.469E-5	0	1.421E-4	0	9.567E-5	0	1.392E-4	0	9.220E-5	0	1.186E-4	0	1.089E-4	0	3.915E-5	0	5.927E-5	0	2.901E-5	0
APS(att48)	1.1		0.6		0.4		0.3		0.2		0.5		0.9		0.2		0.3		0.2		2.7	
lin105+D1	1.486E-3	9	2.260E-3	2	3.171E-3	1	4.186E-3	0	3.311E-3	0	3.114E-3	1	3.076E-3	1	2.629E-3	1	3.368E-3	0	3.525E-3	0	3.355E-3	1
lin105+D2	3.874E-3	7	4.521E-3	4	5.810E-3	0	6.908E-3	0	6.238E-3	0	6.673E-3	0	6.549E-3	0	7.115E-3	0	7.314E-3	0	6.441E-3	0	5.628E-3	0
lin105+D3	1.995E-3	9	3.648E-3	2	5.711E-3	0	5.925E-3	0	5.164E-3	0	4.653E-3	1	3.862E-3	2	7.080E-3	0	3.723E-3	4	6.463E-3	0	5.380E-3	0
lin105+D4	6.441E-4	9	9.110E-4	9	1.929E-3	0	2.308E-3	0	2.062E-3	0	2.105E-3	0	1.854E-3	0	2.292E-3	0	2.021E-3	0	2.419E-3	0	1.685E-3	0
lin105+D5	1.339E-3	10	2.604E-3	7	5.710E-3	0	5.126E-3	0	5.261E-3	0	4.805E-3	0	5.809E-3	0	4.772E-3	0	4.351E-3	0	4.967E-3	0	5.061E-3	0
lin105+D6	2.179E-3	7	2.434E-3	7	4.929E-3	0	3.240E-3	4	6.491E-3	0	4.960E-3	0	5.066E-3	0	5.089E-3	0	5.762E-3	0	6.455E-3	0	3.818E-3	2
lin105+D7	7.137E-4	7	8.890E-4	6	1.253E-3	0	1.209E-3	0	1.470E-3	0	1.672E-3	0	1.564E-3	0	1.362E-3	0	1.098E-3	1	1.370E-3	0	1.782E-3	0
lin105+D8	1.669E-3	9	1.611E-3	9	3.300E-3	0	3.740E-3	0	3.711E-3	0	3.679E-3	0	4.129E-3	0	3.603E-3	0	4.304E-3	0	3.712E-3	0	4.568E-3	0
lin105+D9	2.017E-3	9	1.517E-3	9	5.465E-3	0	5.837E-3	0	4.284E-3	0	4.937E-3	0	5.016E-3	0	3.586E-3	0	3.938E-3	0	5.317E-3	0	4.059E-3	0
lin105+D10	1.074E-3	8	1.498E-3	5	2.593E-3	0	3.242E-3	0	2.546E-3	0	1.962E-3	0	2.788E-3	0	2.181E-3	0	2.323E-3	0	2.643E-3	0	2.261E-3	0
APS(lin105)	8.4		6.0		0.1		0.4		0.0		0.2		0.3		0.1		0.5		0.0		0.3	
a280+D1	1.397E-3	4	1.230E-3	7	1.293E-3	7	1.682E-3	0	1.530E-3	1	1.814E-3	0	1.847E-3	0	1.865E-3	0	1.882E-3	0	1.679E-3	0	1.282E-3	7
a280+D2	1.144E-3	8	1.146E-3	8	1.299E-3	8	2.196E-3	0	2.494E-3	0	2.508E-3	0	2.765E-3	0	2.670E-3	0	2.768E-3	0	2.471E-3	0	2.450E-3	0
a280+D3	1.485E-3	8	9.903E-4	9	1.521E-3	8	3.264E-3	0	2.980E-3	1	3.883E-3	0	4.188E-3	0	3.551E-3	0	3.244E-3	0	2.591E-3	2	3.652E-3	0
a280+D4	8.571E-4	7	9.272E-4	7	9.299E-4	7	1.205E-3	0	1.099E-3	0	1.297E-3	0	1.181E-3	0	1.230E-3	0	1.263E-3	0	1.290E-3	0	8.138E-4	7
a280+D5	9.060E-4	8	9.159E-4	8	1.364E-3	8	2.196E-3	0	2.362E-3	0	2.898E-3	0	1.915E-3	1	2.339E-3	0	2.485E-3	0	2.196E-3	1	1.966E-3	1
a280+D6	1.718E-3	8	1.835E-3	8	2.116E-3	7	3.648E-3	0	3.263E-3	1	3.973E-3	0	4.149E-3	0	3.078E-3	1	3.812E-3	0	3.541E-3	0	3.451E-3	0
a280+D7	4.330E-4	5	4.105E-4	5	5.129E-4	2	6.761E-4	0	5.554E-4	1	6.915E-4	0	6.418E-4	0	5.259E-4	2	5.837E-4	0	7.475E-4	0	7.629E-4	0
a280+D8	8.065E-4	9	9.666E-4	8	1.210E-3	7	2.002E-3	0	2.290E-3	0	2.133E-3	0	2.197E-3	0	1.849E-3	1	1.864E-3	1	2.687E-3	0	1.822E-3	1
a280+D9	5.694E-4	8	6.698E-4	8	7.117E-4	8	1.346E-3	1	1.490E-3	1	1.356E-3	1	1.550E-3	0	1.527E-3	0	1.837E-3	0	1.706E-3	0	2.266E-3	0
a280+D10	4.655E-4	8	6.169E-4	8	4.283E-4	9	1.119E-3	0	1.455E-3	0	1.250E-3	0	1.119E-3	0	1.108E-3	0	1.261E-3	0	1.138E-3	0	1.404E-3	0
APS(a280)	7.3		7.6		7.1		0.1		0.5		0.1		0.1		0.4		0.1		0.3		1.6	
APS(all)	4.5		3.7		2.2		0.3		0.2		0.3		0.4		0.2		0.3		0.2		2.1	

APS is short for Average Performance Score.

TABLE S.XIII
THE RESULTS OF HV OBTAINED BY THE COMPARED ALGORITHMS.

HV	TSPXEA	DNEA-TSP	EAG	DCDG	DYN	NMA
uni1+D1	9.954E-1	9.993E-1 -	9.875E-1 +	9.693E-1 +	9.594E-1 +	9.409E-1 +
uni1+D2	9.846E-1	9.994E-1 -	9.879E-1 -	9.615E-1 +	9.649E-1 +	9.675E-1 +
uni1+D3	9.981E-1	9.993E-1 -	9.773E-1 +	9.793E-1 +	9.594E-1 +	6.964E-1 +
uni1+D4	9.944E-1	9.992E-1 -	9.892E-1 +	9.675E-1 +	9.624E-1 +	9.255E-1 +
uni1+D5	9.943E-1	9.985E-1 -	9.900E-1 +	9.892E-1 +	9.495E-1 +	9.705E-1 +
uni1+D6	9.925E-1	9.983E-1 -	9.892E-1 =	9.662E-1 +	9.430E-1 +	8.711E-1 +
uni1+D7	9.899E-1	9.972E-1 -	9.900E-1 =	9.556E-1 +	9.562E-1 +	4.785E-1 +
uni1+D8	9.930E-1	9.976E-1 -	9.850E-1 =	9.705E-1 +	9.489E-1 +	8.119E-1 +
uni1+D9	9.934E-1	9.961E-1 -	9.863E-1 +	9.640E-1 +	9.545E-1 +	9.671E-1 +
uni1+D10	9.933E-1	9.958E-1 -	9.868E-1 +	9.570E-1 +	9.567E-1 +	9.093E-1 +
+/=/- (uni1)		0/0/10	6/3/1	10/0/0	10/0/0	10/0/0
bays29+D1	9.938E-1	7.936E-1 +	4.657E-2 +	6.853E-1 +	5.136E-1 +	3.981E-1 +
bays29+D2	9.808E-1	7.036E-1 +	3.102E-2 +	5.244E-1 +	3.451E-1 +	4.232E-2 +
bays29+D3	9.980E-1	5.639E-1 +	3.349E-2 +	4.688E-1 +	3.933E-1 +	3.125E-2 +
bays29+D4	9.952E-1	6.157E-1 +	1.593E-1 +	5.000E-1 +	4.715E-1 +	4.929E-1 +
bays29+D5	9.912E-1	7.078E-1 +	1.024E-1 +	2.857E-1 +	4.016E-1 +	1.425E-1 +
bays29+D6	9.896E-1	6.779E-1 +	4.785E-2 +	4.156E-1 +	4.179E-1 +	1.133E-1 +
bays29+D7	9.956E-1	5.421E-1 +	8.026E-2 +	8.144E-1 +	4.771E-1 +	4.752E-1 +
bays29+D8	9.894E-1	5.136E-1 +	4.438E-2 +	3.126E-1 +	3.311E-1 +	6.677E-2 +
bays29+D9	9.923E-1	5.998E-1 +	1.262E-1 +	4.068E-1 +	4.509E-1 +	1.553E-1 +
bays29+D10	9.924E-1	4.465E-1 +	3.569E-2 +	2.490E-1 +	4.096E-1 +	1.746E-1 +
+/=/-(bays29)		10/0/0	10/0/0	10/0/0	10/0/0	10/0/0
att48+D1	9.943E-1	2.163E-1 +	0.000E+0 +	4.142E-1 +	2.038E-2 +	0.000E+0 +
att48+D2	9.826E-1	9.667E-2 +	0.000E+0 +	2.442E-1 +	0.000E+0 +	0.000E+0 +
att48+D3	9.948E-1	1.302E-1 +	0.000E+0 +	4.019E-1 +	2.370E-3 +	0.000E+0 +
att48+D4	9.949E-1	2.554E-1 +	1.278E-2 +	4.642E-1 +	2.012E-2 +	0.000E+0 +
att48+D5	9.871E-1	7.083E-2 +	0.000E+0 +	2.809E-1 +	0.000E+0 +	0.000E+0 +
att48+D6	9.871E-1	5.647E-2 +	0.000E+0 +	2.016E-1 +	0.000E+0 +	0.000E+0 +
att48+D7	9.949E-1	2.045E-1 +	3.799E-3 +	4.295E-1 +	1.879E-2 +	0.000E+0 +
att48+D8	9.869E-1	8.465E-2 +	0.000E+0 +	1.360E-1 +	0.000E+0 +	0.000E+0 +
att48+D9	9.905E-1	1.707E-1 +	0.000E+0 +	1.297E-1 +	2.203E-3 +	0.000E+0 +
att48+D10	9.912E-1	1.121E-1 +	7.184E-4 +	1.118E-1 +	0.000E+0 +	0.000E+0 +
+/=/-(att48)		10/0/0	10/0/0	10/0/0	10/0/0	10/0/0
lin105+D1	9.704E-1	0.000E+0 +	0.000E+0 +	3.725E-2 +	0.000E+0 +	0.000E+0 +
lin105+D2	9.157E-1	0.000E+0 +	0.000E+0 +	3.065E-2 +	0.000E+0 +	0.000E+0 +
lin105+D3	9.613E-1	0.000E+0 +	0.000E+0 +	6.215E-3 +	0.000E+0 +	0.000E+0 +
lin105+D4	9.851E-1	0.000E+0 +	0.000E+0 +	5.471E-2 +	0.000E+0 +	0.000E+0 +
lin105+D5	9.701E-1	0.000E+0 +	0.000E+0 +	5.228E-2 +	0.000E+0 +	0.000E+0 +
lin105+D6	9.520E-1	0.000E+0 +	0.000E+0 +	7.157E-3 +	0.000E+0 +	0.000E+0 +
lin105+D7	9.807E-1	0.000E+0 +	0.000E+0 +	1.205E-1 +	0.000E+0 +	0.000E+0 +
lin105+D8	9.634E-1	0.000E+0 +	0.000E+0 +	2.927E-2 +	0.000E+0 +	0.000E+0 +
lin105+D9	9.511E-1	0.000E+0 +	0.000E+0 +	1.405E-2 +	0.000E+0 +	0.000E+0 +
lin105+D10	9.700E-1	0.000E+0 +	0.000E+0 +	5.436E-2 +	0.000E+0 +	0.000E+0 +
+/=/-(lin105)		10/0/0	10/0/0	10/0/0	10/0/0	10/0/0

TABLE S.XIV
THE RESULTS OF GD OBTAINED BY THE COMPARED ALGORITHMS.

GD	TSPXEA	DNEA-TSP	EAG	DCDG	DYN	NMA
uni1+D1	3.644E-4	2.148E-5 -	6.858E-4 +	7.642E-4 +	2.028E-3 +	5.125E-6 -
uni1+D2	1.505E-3	1.762E-6 -	1.248E-3 -	0.000E+0 -	1.420E-3 =	0.000E+0 -
uni1+D3	2.363E-4	0.000E+0 -	1.443E-3 +	1.005E-4 -	1.515E-3 +	0.000E+0 -
uni1+D4	4.788E-4	1.886E-5 -	6.194E-4 =	7.517E-4 =	1.467E-3 +	1.146E-6 -
uni1+D5	1.038E-4	0.000E+0 -	3.754E-4 +	1.339E-4 +	1.232E-3 +	0.000E+0 -
uni1+D6	3.443E-4	2.630E-5 -	3.763E-4 =	6.423E-6 -	2.988E-3 +	0.000E+0 -
uni1+D7	5.984E-4	0.000E+0 -	1.132E-4 -	4.924E-5 -	7.455E-4 =	0.000E+0 -
uni1+D8	2.806E-4	7.256E-5 -	5.983E-4 =	1.448E-4 -	1.271E-3 +	3.540E-6 -
uni1+D9	0.000E+0	0.000E+0 =	3.681E-4 +	2.080E-4 =	8.096E-4 +	0.000E+0 =
uni1+D10	8.547E-5	0.000E+0 =	1.221E-3 +	3.402E-5 =	6.612E-4 +	0.000E+0 =
+/=/- (uni1)		0/2/8	5/3/2	2/3/5	8/2/0	0/2/8
bays29+D1	3.543E-4	1.248E-2 +	2.211E-1 +	3.884E-2 +	5.100E-2 +	1.072E-1 +
bays29+D2	1.354E-3	3.028E-2 +	4.583E-1 +	9.179E-2 +	7.333E-2 +	3.119E-1 +
bays29+D3	5.390E-5	7.367E-2 +	6.256E-1 +	1.587E-1 +	8.893E-2 +	3.614E-1 +
bays29+D4	1.997E-4	3.925E-2 +	2.278E-1 +	7.339E-2 +	7.114E-2 +	7.326E-2 +
bays29+D5	3.588E-4	2.892E-2 +	3.788E-1 +	1.244E-1 +	1.069E-1 +	2.312E-1 +
bays29+D6	3.831E-4	5.181E-2 +	4.236E-1 +	1.626E-1 +	8.223E-2 +	2.675E-1 +
bays29+D7	1.557E-5	4.463E-2 +	2.244E-1 +	2.137E-2 +	4.906E-2 +	7.244E-2 +
bays29+D8	4.874E-4	1.347E-1 +	6.588E-1 +	2.612E-1 +	1.258E-1 +	2.708E-1 +
bays29+D9	8.017E-5	3.974E-2 +	2.546E-1 +	7.777E-2 +	6.041E-2 +	1.781E-1 +
bays29+D10	1.813E-5	5.852E-2 +	2.937E-1 +	1.008E-1 +	8.124E-2 +	1.560E-1 +
+/=/-(bays29)		10/0/0	10/0/0	10/0/0	10/0/0	10/0/0
att48+D1	3.671E-4	1.150E-1 +	9.976E-1 +	1.084E-1 +	3.546E-1 +	9.348E-1 +
att48+D2	1.079E-3	1.935E-1 +	1.947E+0 +	1.995E-1 +	5.584E-1 +	1.813E+0 +
att48+D3	2.138E-4	2.575E-1 +	2.752E+0 +	1.935E-1 +	1.095E+0 +	2.093E+0 +
att48+D4	2.357E-4	8.518E-2 +	7.602E-1 +	6.743E-2 +	3.412E-1 +	5.297E-1 +
att48+D5	5.051E-4	3.524E-1 +	2.144E+0 +	2.051E-1 +	7.789E-1 +	2.135E+0 +
att48+D6	4.237E-4	3.725E-1 +	2.356E+0 +	2.691E-1 +	1.065E+0 +	2.407E+0 +
att48+D7	3.358E-5	1.078E-1 +	8.639E-1 +	7.611E-2 +	3.350E-1 +	5.719E-1 +
att48+D8	5.577E-4	3.451E-1 +	3.167E+0 +	3.738E-1 +	1.171E+0 +	2.412E+0 +
att48+D9	1.544E-4	1.646E-1 +	1.678E+0 +	2.512E-1 +	7.186E-1 +	1.713E+0 +
att48+D10	8.640E-5	2.106E-1 +	1.653E+0 +	2.165E-1 +	5.919E-1 +	1.367E+0 +
+/=/-(att48)		10/0/0	10/0/0	10/0/0	10/0/0	10/0/0
lin105+D1	1.486E-3	6.698E+0 +	1.456E+1 +	4.419E-1 +	7.976E+0 +	1.933E+1 +
lin105+D2	3.874E-3	1.024E+1 +	2.315E+1 +	4.756E-1 +	1.297E+1 +	3.259E+1 +
lin105+D3	1.995E-3	1.025E+1 +	2.644E+1 +	7.304E-1 +	1.501E+1 +	3.365E+1 +
lin105+D4	6.441E-4	2.731E+0 +	7.935E+0 +	2.855E-1 +	4.923E+0 +	1.164E+1 +
lin105+D5	1.339E-3	8.627E+0 +	2.056E+1 +	3.946E-1 +	1.301E+1 +	3.144E+1 +
lin105+D6	2.179E-3	1.129E+1 +	2.239E+1 +	5.281E-1 +	1.301E+1 +	3.447E+1 +
lin105+D7	7.137E-4	2.816E+0 +	6.724E+0 +	2.129E-1 +	4.178E+0 +	9.737E+0 +
lin105+D8	1.669E-3	8.513E+0 +	2.041E+1 +	6.618E-1 +	1.088E+1 +	2.579E+1 +
lin105+D9	2.017E-3	8.949E+0 +	1.901E+1 +	6.466E-1 +	1.112E+1 +	3.014E+1 +
lin105+D10	1.074E-3	5.535E+0 +	1.186E+1 +	3.382E-1 +	7.461E+0 +	1.828E+1 +
+/=/-(lin105)		10/0/0	10/0/0	10/0/0	10/0/0	10/0/0

TABLE S.XV
THE RESULTS OF IGD OBTAINED BY THE COMPARED ALGORITHMS.

IGD	TSPXEA	DNEA-TSP	EAG	DCDG	DYN	NMA
uni1+D1	3.196E-3	4.610E-4 -	6.303E-3 +	2.418E-2 +	2.091E-2 +	4.755E-2 +
uni1+D2	7.354E-3	2.411E-4 -	6.731E-3 =	2.605E-2 +	1.695E-2 +	2.714E-2 +
uni1+D3	1.911E-3	1.033E-3 -	8.562E-3 +	2.037E-2 +	1.618E-2 +	2.489E-1 +
uni1+D4	4.630E-3	7.129E-4 -	5.857E-3 +	2.477E-2 +	1.882E-2 +	6.428E-2 +
uni1+D5	4.000E-3	1.274E-3 -	6.933E-3 +	8.674E-3 +	1.999E-2 +	2.327E-2 +
uni1+D6	4.467E-3	1.340E-3 -	7.721E-3 +	2.168E-2 +	2.595E-2 +	7.884E-2 +
uni1+D7	4.022E-3	1.913E-3 -	5.001E-3 +	2.620E-2 +	1.898E-2 +	3.126E-1 +
uni1+D8	4.505E-3	2.314E-3 -	5.621E-3 =	2.240E-2 +	1.839E-2 +	1.787E-1 +
uni1+D9	4.133E-3	2.619E-3 -	4.986E-3 +	2.121E-2 +	1.465E-2 +	1.161E-2 +
uni1+D10	4.395E-3	2.987E-3 -	5.290E-3 +	2.509E-2 +	1.353E-2 +	3.741E-2 +
+/=/- (uni1)		0/0/10	8/2/0	10/0/0	10/0/0	10/0/0
bays29+D1	4.263E-3	1.274E-1 +	1.840E+0 +	2.729E-1 +	2.713E-1 +	3.198E-1 +
bays29+D2	9.119E-3	2.905E-1 +	2.638E+0 +	6.638E-1 +	3.798E-1 +	6.541E-1 +
bays29+D3	2.360E-3	7.532E-1 +	4.083E+0 +	1.017E+0 +	5.251E-1 +	7.657E-1 +
bays29+D4	4.027E-3	3.905E-1 +	1.702E+0 +	5.483E-1 +	3.160E-1 +	2.458E-1 +
bays29+D5	5.706E-3	2.883E-1 +	2.543E+0 +	1.073E+0 +	4.368E-1 +	5.245E-1 +
bays29+D6	5.410E-3	5.244E-1 +	3.672E+0 +	1.163E+0 +	4.818E-1 +	5.667E-1 +
bays29+D7	3.082E-3	4.365E-1 +	1.808E+0 +	1.656E-1 +	2.361E-1 +	2.348E-1 +
bays29+D8	6.371E-3	1.379E+0 +	5.775E+0 +	2.120E+0 +	5.830E-1 +	6.363E-1 +
bays29+D9	4.147E-3	3.899E-1 +	2.093E+0 +	6.946E-1 +	2.835E-1 +	4.538E-1 +
bays29+D10	4.786E-3	5.408E-1 +	2.144E+0 +	7.952E-1 +	3.555E-1 +	4.301E-1 +
+/=/-(bays29)		10/0/0	10/0/0	10/0/0	10/0/0	10/0/0
att48+D1	4.232E-3	1.048E+0 +	4.472E+0 +	8.440E-1 +	1.452E+0 +	1.777E+0 +
att48+D2	8.883E-3	1.418E+0 +	6.890E+0 +	1.587E+0 +	1.792E+0 +	2.808E+0 +
att48+D3	3.729E-3	1.936E+0 +	9.045E+0 +	1.496E+0 +	3.335E+0 +	3.181E+0 +
att48+D4	3.885E-3	7.569E-1 +	3.263E+0 +	5.361E-1 +	1.305E+0 +	1.190E+0 +
att48+D5	6.951E-3	2.489E+0 +	7.429E+0 +	1.805E+0 +	2.490E+0 +	3.088E+0 +
att48+D6	7.258E-3	2.886E+0 +	9.809E+0 +	2.248E+0 +	3.832E+0 +	3.622E+0 +
att48+D7	3.446E-3	8.840E-1 +	3.595E+0 +	6.555E-1 +	1.158E+0 +	1.247E+0 +
att48+D8	7.193E-3	2.857E+0 +	1.080E+1 +	3.113E+0 +	3.915E+0 +	3.844E+0 +
att48+D9	4.908E-3	1.411E+0 +	7.349E+0 +	2.041E+0 +	2.673E+0 +	2.568E+0 +
att48+D10	4.755E-3	1.663E+0 +	5.988E+0 +	1.794E+0 +	2.112E+0 +	2.251E+0 +
+/=/-(att48)		10/0/0	10/0/0	10/0/0	10/0/0	10/0/0
lin105+D1	1.559E-2	1.345E+1 +	2.869E+1 +	4.471E+0 +	1.877E+1 +	2.355E+1 +
lin105+D2	3.626E-2	2.018E+1 +	4.177E+1 +	4.734E+0 +	2.876E+1 +	3.564E+1 +
lin105+D3	2.093E-2	2.160E+1 +	5.192E+1 +	7.341E+0 +	3.000E+1 +	3.843E+1 +
lin105+D4	7.984E-3	7.889E+0 +	1.733E+1 +	2.861E+0 +	1.120E+1 +	1.502E+1 +
lin105+D5	1.567E-2	1.810E+1 +	4.251E+1 +	3.942E+0 +	2.776E+1 +	3.274E+1 +
lin105+D6	2.360E-2	2.066E+1 +	4.804E+1 +	5.276E+0 +	2.951E+1 +	3.611E+1 +
lin105+D7	8.869E-3	7.227E+0 +	1.424E+1 +	2.140E+0 +	9.192E+0 +	1.258E+1 +
lin105+D8	1.791E-2	1.670E+1 +	3.597E+1 +	6.680E+0 +	2.450E+1 +	3.059E+1 +
lin105+D9	2.233E-2	1.732E+1 +	3.886E+1 +	6.453E+0 +	2.455E+1 +	3.311E+1 +
lin105+D10	1.320E-2	1.143E+1 +	2.421E+1 +	3.375E+0 +	1.617E+1 +	2.058E+1 +
+/=/-(lin105)		10/0/0	10/0/0	10/0/0	10/0/0	10/0/0

TABLE S.XVI
THE RESULTS OF IGDX OBTAINED BY THE COMPARED ALGORITHMS.

IGDX	TSPXEA	DNEA-TSP	EAG	DCDG	DYN	NMA
uni1+D1	1.295E-1	1.168E-1 -	1.641E-1 +	2.633E-1 +	2.334E-1 +	2.361E-1 +
uni1+D2	1.420E-1	1.171E-1 -	1.554E-1 +	2.338E-1 +	1.950E-1 +	1.725E-1 +
uni1+D3	1.166E-1	1.187E-1 +	1.630E-1 +	2.378E-1 +	1.964E-1 +	3.381E-1 +
uni1+D4	1.720E-1	1.541E-1 -	1.871E-1 +	2.738E-1 +	2.365E-1 +	2.559E-1 +
uni1+D5	1.569E-1	1.563E-1 =	1.737E-1 +	1.946E-1 +	2.085E-1 +	1.780E-1 +
uni1+D6	1.691E-1	1.644E-1 -	1.799E-1 +	2.446E-1 +	2.392E-1 +	2.996E-1 +
uni1+D7	1.854E-1	1.892E-1 +	2.032E-1 +	2.883E-1 +	2.315E-1 +	4.009E-1 +
uni1+D8	2.265E-1	2.081E-1 -	2.280E-1 =	3.056E-1 +	2.526E-1 +	3.752E-1 +
uni1+D9	2.056E-1	2.079E-1 +	2.323E-1 +	2.986E-1 +	2.424E-1 +	2.246E-1 +
uni1+D10	2.212E-1	2.252E-1 +	2.388E-1 +	3.189E-1 +	2.557E-1 +	3.079E-1 +
+/=/- (uni1)		4/1/5	9/1/0	10/0/0	10/0/0	10/0/0
bays29+D1	6.197E-2	2.807E-1 +	3.856E-1 +	2.377E-1 +	4.298E-1 +	4.396E-1 +
bays29+D2	3.852E-2	2.439E-1 +	3.843E-1 +	2.495E-1 +	3.733E-1 +	4.456E-1 +
bays29+D3	3.699E-2	2.504E-1 +	3.937E-1 +	2.527E-1 +	3.438E-1 +	4.453E-1 +
bays29+D4	4.684E-2	2.976E-1 +	3.835E-1 +	2.648E-1 +	4.717E-1 +	4.505E-1 +
bays29+D5	5.003E-2	2.625E-1 +	3.860E-1 +	2.695E-1 +	3.819E-1 +	4.385E-1 +
bays29+D6	6.119E-2	2.588E-1 +	3.872E-1 +	2.827E-1 +	3.588E-1 +	4.489E-1 +
bays29+D7	5.275E-2	3.298E-1 +	4.175E-1 +	2.585E-1 +	4.485E-1 +	4.615E-1 +
bays29+D8	7.914E-2	2.911E-1 +	4.033E-1 +	2.937E-1 +	4.096E-1 +	4.706E-1 +
bays29+D9	6.689E-2	2.689E-1 +	3.574E-1 +	2.569E-1 +	3.954E-1 +	4.519E-1 +
bays29+D10	6.426E-2	2.983E-1 +	3.999E-1 +	2.787E-1 +	4.091E-1 +	4.644E-1 +
+/=/-(bays29)		10/0/0	10/0/0	10/0/0	10/0/0	10/0/0
att48+D1	2.867E-2	4.741E-1 +	4.837E-1 +	3.194E-1 +	5.816E-1 +	6.077E-1 +
att48+D2	3.571E-2	4.509E-1 +	4.590E-1 +	3.006E-1 +	5.610E-1 +	5.894E-1 +
att48+D3	4.215E-2	4.479E-1 +	4.860E-1 +	2.953E-1 +	5.802E-1 +	5.984E-1 +
att48+D4	3.281E-2	4.821E-1 +	4.945E-1 +	3.248E-1 +	6.054E-1 +	6.086E-1 +
att48+D5	5.424E-2	4.525E-1 +	4.699E-1 +	2.914E-1 +	5.600E-1 +	6.027E-1 +
att48+D6	5.069E-2	4.450E-1 +	4.805E-1 +	3.312E-1 +	5.636E-1 +	6.069E-1 +
att48+D7	4.235E-2	4.840E-1 +	4.662E-1 +	3.067E-1 +	6.078E-1 +	6.150E-1 +
att48+D8	7.642E-2	4.290E-1 +	4.953E-1 +	3.388E-1 +	5.935E-1 +	6.106E-1 +
att48+D9	5.019E-2	4.454E-1 +	4.957E-1 +	3.109E-1 +	5.839E-1 +	6.082E-1 +
att48+D10	4.724E-2	4.362E-1 +	4.950E-1 +	3.114E-1 +	5.748E-1 +	6.041E-1 +
+/=/-(att48)		10/0/0	10/0/0	10/0/0	10/0/0	10/0/0
lin105+D1	3.816E-2	7.146E-1 +	5.854E-1 +	2.376E-1 +	7.810E-1 +	7.038E-1 +
lin105+D2	3.354E-2	7.025E-1 +	5.960E-1 +	2.303E-1 +	7.958E-1 +	7.051E-1 +
lin105+D3	3.136E-2	6.956E-1 +	6.054E-1 +	2.366E-1 +	7.904E-1 +	7.050E-1 +
lin105+D4	3.296E-2	7.049E-1 +	5.908E-1 +	2.486E-1 +	7.934E-1 +	7.047E-1 +
lin105+D5	3.140E-2	7.129E-1 +	5.851E-1 +	2.486E-1 +	7.898E-1 +	7.055E-1 +
lin105+D6	3.679E-2	7.149E-1 +	5.889E-1 +	2.460E-1 +	7.892E-1 +	7.015E-1 +
lin105+D7	3.655E-2	7.202E-1 +	5.871E-1 +	2.292E-1 +	7.909E-1 +	7.041E-1 +
lin105+D8	4.103E-2	7.130E-1 +	5.905E-1 +	2.514E-1 +	7.982E-1 +	7.068E-1 +
lin105+D9	3.486E-2	7.229E-1 +	5.928E-1 +	2.452E-1 +	7.774E-1 +	7.109E-1 +
lin105+D10	4.798E-2	7.076E-1 +	5.919E-1 +	2.539E-1 +	7.923E-1 +	7.061E-1 +
+/=/-(lin105)		10/0/0	10/0/0	10/0/0	10/0/0	10/0/0